Advanced Drug Delivery Reviews xxx (2015) xxx–xxx

Contents lists available at ScienceDirect

Advanced Drug Delivery Reviews

journal homepage: www.elsevier.com/locate/addr

# Radioimmunotherapy of cancer with high linear energy transfer (LET) radiation delivered by radionuclides emitting α-particles or Auger electrons☆

Sadaf Aghevlian [a,1], Amanda J. Boyle [a,1], Raymond M. Reilly [a,b,c,*]

[a] Department of Pharmaceutical Sciences, University of Toronto, Toronto, ON, Canada
[b] Department of Medical Imaging, University of Toronto, Toronto, ON, Canada
[c] Toronto General Research Institute and Joint Department of Medical Imaging, University Health Network, Toronto, ON, Canada

ARTICLE INFO

*Article history:*
Received 12 October 2015
Received in revised form 26 November 2015
Accepted 6 December 2015
Available online xxxx

*Keywords:*
Radioimmunotherapy
α-Particles
Auger electrons
Radiation treatment
Monoclonal antibodies
Cancer

ABSTRACT

Radioimmunotherapy (RIT) aims to selectively deliver radionuclides emitting α-particles, β-particles or Auger electrons to tumors by conjugation to monoclonal antibodies (mAbs) that recognize tumor-associated antigens/receptors. The approach has been most successful for treatment of non-Hodgkin's B-cell lymphoma but challenges have been encountered in extending these promising results to the treatment of solid malignancies. These challenges include the low potency of β-particle emitters such as $^{131}$I, $^{177}$Lu or $^{90}$Y which have been commonly conjugated to the mAbs, due to their low linear energy transfer (LET = 0.1–1.0 keV/μm). Furthermore, since the β-particles have a 2–10 mm range, there has been dose-limiting non-specific toxicity to hematopoietic stem cells in the bone marrow (BM) due to the cross-fire effect. Conjugation of mAbs to α-particle-emitters (e.g. $^{225}$Ac, $^{213}$Bi, $^{212}$Pb or $^{211}$At) or Auger electron-emitters (e.g. $^{111}$In, $^{67}$Ga, $^{123}$I or $^{125}$I) would increase the potency of RIT due to their high LET (50–230 keV/μm and 4 to 26 keV/μm, respectively). In addition, α-particles have a range in tissues of 28–100 μm and Auger electrons are nanometer in range which greatly reduces or eliminates the cross-fire effect compared to β-particles, potentially reducing their non-specific toxicity to the BM. In this review, we describe the results of preclinical and clinical studies of RIT of cancer using radioimmunoconjugates emitting α-particles or Auger electrons, and discuss the potential of these high LET forms of radiation to improve the outcome of cancer patients.



**Contents**



☆ This review is part of the *Advanced Drug Delivery Reviews* theme issue on "Radiotherapy for Cancer: Present and Future".

* Corresponding author at: Leslie Dan Faculty of Pharmacy, University of Toronto, 144 College St., Toronto, Ontario M5S 3M2, Canada.
*E-mail address:* raymond.reilly@utoronto.ca (R.M. Reilly).

[1] Equal contributions from both authors.

http://dx.doi.org/10.1016/j.addr.2015.12.003
0169-409X/

## 1. Introduction

Radioimmunotherapy (RIT) aims to selectively deliver radiation to tumors using radionuclides that emit α-particles, β-particles or Auger electrons conjugated to monoclonal antibodies (mAbs) that recognize tumor-associated antigens/receptors (Fig. 1) [1]. RIT has been studied for more than three decades and several important conclusions have emerged. Firstly, proof-of-principle demonstrating the effectiveness of RIT for cancer treatment has been repeatedly and clearly shown in numerous tumor xenograft mouse models and employing different mAbs that target a wide range of tumor phenotypes and using a variety of radionuclides. Secondly, these promising preclinical results have been advanced successfully to treatment of patients with hematological malignancies, especially non-Hodgkin's B-cell lymphoma (NHL) resulting in the regulatory approval and introduction into clinical practice of two RIT agents: $^{131}$I-tositumomab (Bexxar) and $^{90}$Y-ibritumomab tiuxetan (Zevalin) [2,3]. Thirdly, the encouraging results from preclinical studies of RIT of solid tumors have proven more difficult to extend to successful RIT of these tumors in humans [1]. Several obstacles have been identified. The low potency of the β-particles emitted by $^{131}$I, $^{90}$Y, $^{177}$Lu, $^{186}$Re or $^{188}$Re which have been commonly linked to the mAbs combined with the low tumor uptake of radiolabeled mAbs in humans [<0.1% injected dose/g (% ID/g)] restricted the radiation absorbed dose deposited in tumors and the effectiveness of RIT. Furthermore, the long range (2–10 mm) of the emitted β-particles combined with the persistence of radiolabeled mAbs in the blood caused "cross-fire" non-specific irradiation of hematopoietic stem cells in the bone marrow (BM) (Fig. 2) which limited the dose of radioactivity that could be safely administered to patients, further limiting the effectiveness of RIT. Finally, the immunogenicity of murine and chimeric mAbs which were employed in the early studies of RIT in humans prevented dose-fractionation to minimize BM toxicity or re-treatment to improve patient outcomes. Advances in recombinant engineering of mAbs have now made available humanized and fully-human mAbs which are essentially non-immunogenic in humans and would permit multiple fractionated doses of radiolabeled mAbs to be administered in RIT to allow re-treatment [4].

The low linear energy transfer (LET) of β-particles results in relatively low deposition of energy in tumor cells restricting the potency for killing these cells. LET describes the energy deposited over the track length of the radiation in tissues. Most β-particles have LET of 0.1–1.0 keV/μm. In contrast, α-particles have LET values of 50–230 keV/μm and Auger electrons have LET of 4 to 26 keV/μm, which would render these forms of radiation more cytotoxic (Fig. 3). Moreover, α-particles have a range of only 50–100 μm, which restricts their cross-fire effect to 5–10 cell diameters, in contrast to β-particles which irradiate up to 200–1000 cell diameters from the site of decay (Fig. 3). The subcellular nanometer range of Auger electrons eliminates the cross-fire effect and requires that these electrons be released in close proximity to nuclear DNA to cause lethal double-strand breaks (DSBs). Due to their potentially greater potency and lower non-specific toxicity to non-targeted normal tissues including the BM, α-particle and Auger electron-emitting radionuclides are highly attractive for RIT of malignancies. However, their short range makes these forms of radiation most suitable for eradicating single cells and small volume disease (<1 cm diameter) whereas the longer range of β-particles makes this form of radiation more feasible for treating larger tumor masses (>1 cm) [5]. In this review, we describe the results of preclinical and clinical studies of RIT of cancer using radioimmunoconjugates (RICs) emitting α-particles or Auger electrons, and discuss the potential of these high LET forms of radiation to improve the outcome of cancer patients.

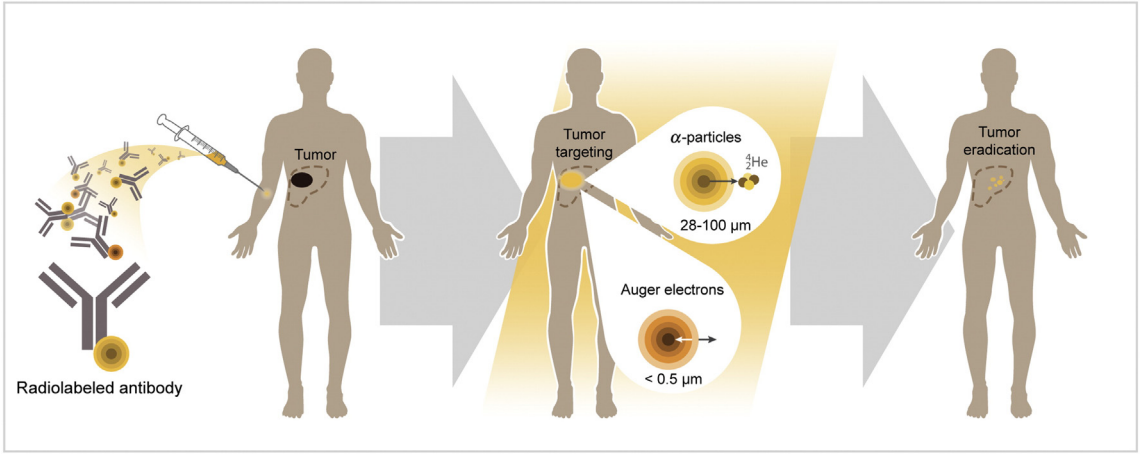


**Fig. 1.** Concept for radioimmunotherapy of cancer using monoclonal antibodies labeled with high linear energy transfer (LET) α-particle-emitting with a range of 28–100 μm or Auger electron-emitting radionuclides with a range <0.5 μm.

Please cite this article as: S. Aghevlian, et al., Radioimmunotherapy of cancer with high linear energy transfer (LET) radiation delivered by radionuclides emitting α-particles or ..., Adv. Drug Deliv. Rev. (2015), http://dx.doi.org/10.1016/j.addr.2015.12.003

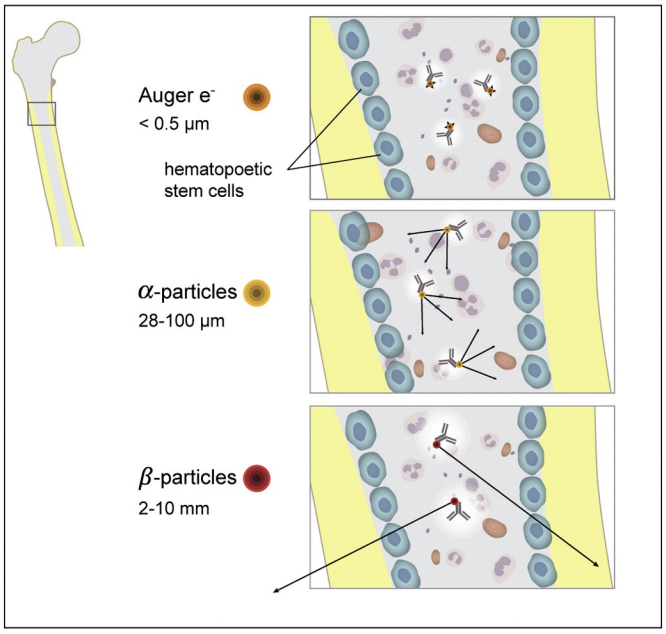


**Fig. 2.** The cross-fire effect of the 2–10 mm range β-particles emitted by circulating radiolabeled monoclonal antibodies perfusing the bone marrow (BM) decreases the viability of hematopoietic stem cells resulting in myelosuppression. In contrast, α-particles have a range of only 28–100 μm and Auger electrons have a range <0.5 μm which greatly reduces or eliminates the BM toxicity of radioimmunotherapy.

## 2. Radioimmunotherapy (RIT) with α-particles

### *2.1. Properties of α-particles*

An α-particle is a helium-4 ($^4$He) nucleus consisting of two protons and two neutrons which carries a +2 charge (Fig. 4). α-Particles have much higher LET (50–230 keV/μm) than β-particles emitted by radionuclides such as $^{131}$I, $^{90}$Y, $^{177}$Lu, $^{186}$Re or $^{188}$Re (LET = 0.1–1.0 keV/μm) due to their short range in tissues (28–100 μm; Fig. 3) [6]. The range of α-particles in tissues corresponds to only 5–10 cell diameters, which restricts the deposition of radiation to the targeted cell and closely neighboring cells. In contrast, β-particles deposit their energy along a track

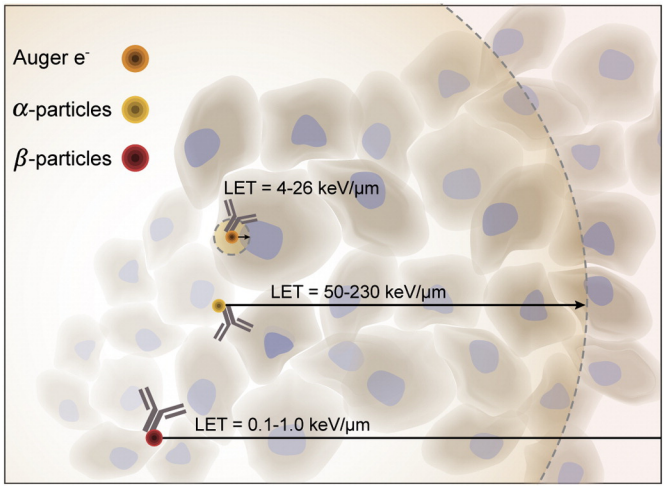


**Fig. 3.** Illustration of the track of α-particles, β-particles or Auger electrons emitted by radiolabeled monoclonal antibodies targeted to cancer cells. The short track length of α-particles (28–100 μm) and Auger electrons (<0.5 μm) results in high linear energy transfer (LET) values of 50–230 keV/μm and 4 to 26 keV/μm, respectively. β-Particles have a track length of 2–10 mm resulting in LET of 0.1–1.0 keV/μm. The high LET of α-particles (50–100 μm) and Auger electrons makes these forms of radiation more powerful for killing cancer cells than β-particles.

that greatly exceeds the diameter of a single targeted cell [7,8]. The high LET and short range of α-particles make this form of radiation useful for eradicating circulating malignant cells (e.g. leukemia cells in the blood or BM) or small clusters of cells (e.g. disseminated disease and micrometastases from solid tumors). Indeed, it has been shown that α-emitters are more effective than β-emitters for RIT of small lung metastases in rats, providing greater relative biological effectiveness (RBE) [9,10]. RBE describes the effectiveness of a particular type of radiation for causing an effect (e.g. cytotoxicity) compared to X- or γ-radiation. A high RBE is desirable for RIT. The decay scheme of some α-emitters (e.g. $^{225}$Ac and $^{225}$Ra; Fig. 5) yields daughter products that are α-emitters or β-emitters, and such radionuclides have been proposed as α-particle "radionuclide generator systems" that could deliver a higher radiation absorbed dose to tumors than radionuclides that emit only single α-particles or decay to stable elements or daughter products that emit radiation with lower RBE (e.g. β-particles, X- or γ-radiation) [11]. Although there is great potential with the radionuclide generator concept, a limitation is that the daughter α-emitters in most cases will not remain complexed to chelators substituted onto the mAb since they represent elements with different chemistry. In addition, the high recoil energy upon decay also promotes their release from the chelators (Fig. 6). Release of daughter radionuclides and their redistribution to normal tissues have been reported for the α-emitter $^{225}$Ac which decays to several daughter radionuclides, including $^{213}$Bi, which is also an α-emitter. Redistribution of $^{213}$Bi released from $^{225}$Ac-labeled anti-CD33 mAb HuM195 deposited α-radiation in the kidneys causing acute renal dysfunction in non-human primates [12,13]. This phenomenon has not been confirmed in humans however, since early results of a Phase I clinical trial of $^{225}$Ac-labeled HuM195 (ClinicalTrials.gov identifier NCT00672165) in patients with acute myeloid leukemia (AML) presented at the annual meeting of the American Society of Clinical Oncology (ASCO) in 2015 indicated that the maximum tolerated dose (MTD) was not yet reached [14].

### *2.2. Radiobiological effects of α-particles*

The RBE of α-particles ranges from 3 to 7, indicating that at the same radiation absorbed dose, the biological effects of α-particles are 3 to 7 times greater than for β-radiation which has an RBE of 1 [15]. The primary target of α-particles in causing cell death is considered to be nuclear DNA, and is manifested by DNA double-strand breaks (DSBs). Studies have shown that when the track of an α-particle traverses the cytoplasm, there fails to be a lethal effect on a cell, while a track that crosses the nucleus is correlated with cytotoxicity [16]. A single track of ionizing radiation from an α-emitter induces clusters of DNA DSBs, which can be detected in vitro by immunofluorescence probing for phosphorylated histone 2A which accumulates at sites of unrepaired DNA DSBs [6]. Importantly, the induction of DSBs by α-particles is independent of tissue oxygenation, which is advantageous compared to β-emitters for RIT which rely on formation of oxygen free radicals to indirectly damage DNA [6,17]. Hypoxia is a common resistance mechanism to treatment of cancer with low LET radiation [18]. High LET radiation such as α-particles directly cleaves the DNA duplex, which does not rely on tumor oxygenation. Wulbrand et al. found that $^{213}$Bi-labeled anti-epidermal growth factor receptor (EGFR) mAb matuzumab, killed hypoxic CAL 33 squamous cell carcinoma cells as effectively as normoxic cells in vitro [17]. The mechanism of cell death from RIT with α-emitters was examined in one report in which intraperitoneally (i.p.) injected $^{212}$Pb-labeled anti-human epidermal growth factor receptor-2 (HER2) mAb, trastuzumab, was compared to non-specific $^{212}$Pb-human IgG in mice with disseminated i.p. LS-174 T human colon cancer tumors [19]. Ex vivo examination of these tumors revealed that these HER2-targeted RICs caused increased apoptosis and DNA DSBs, delayed DNA damage repair, and caused G2-M cell cycle arrest compared to treatment with control irrelevant RICs.

It is important to consider the effects of α-particle RIT on toxicity to normal organs, especially for $^{211}$At-labeled mAbs which may undergo

Please cite this article as: S. Aghevlian, et al., Radioimmunotherapy of cancer with high linear energy transfer (LET) radiation delivered by radionuclides emitting α-particles or ..., Adv. Drug Deliv. Rev. (2015), http://dx.doi.org/10.1016/j.addr.2015.12.003

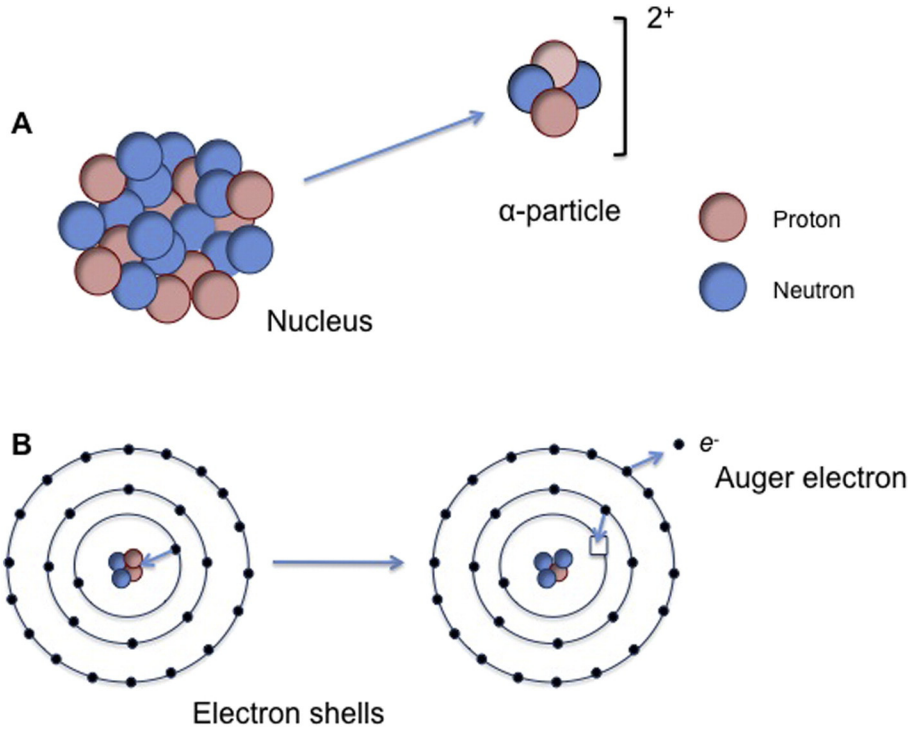


**Fig. 4.** (A) α-particles are high energy (several MeV) radiation composed of two protons and two neutrons and carry a $2^+$ charge. (B) Auger electrons are very low energy (<25 keV) electrons with a $1^-$ charge emitted by radionuclides that decay by electron capture (EC). In EC, a proton in the nucleus captures an electron from an inner orbital shell converting the proton to a neutron. This creates a vacancy in the shell which is filled by an electron from a higher shell, creating a subsequent vacancy, which is then filled by decay of an electron from a higher shell etc. Ultimately, the energy released from these electron transitions is imparted on an outer orbital electron which is ejected from the atom (Auger electron), creating a transiently positively-charged nucleus.

de-astatination in vivo. Free $^{211}$At accumulates in the thyroid unless blocked by potassium perchlorate administration [20]. In a Phase I clinical trial in 9 patients with ovarian cancer administered $^{211}$At-MX35 F(ab′)$_2$ fragments recognizing sodium-dependent phosphate transport protein 2b (NaPi2b), therapeutic radiation absorbed doses were deposited in tumors without toxicity to normal tissues, including the thyroid, by co-administering RIT with potassium perchlorate [21].

### 2.3. Selection of an α-emitter for RIT

Several α-emitting radionuclides have been studied for RIT (Table 1). Important considerations in selecting an α-emitter for RIT include its availability, the chemistry for radiolabeling mAbs, the physical half-life ($t_{1/2}$p), and the decay scheme, particularly the formation of daughter products that emit α- or β-radiation that could redistribute from the tumor to normal tissues, potentially causing "off-target" normal tissue toxicity. The availability of $^{211}$At has been limited due to the few high energy cyclotrons worldwide capable of $^{211}$At production. The most common mode for production of $^{211}$At is irradiation of a bismuth target, $^{209}$Bi(α,2n)$^{211}$At, in which α-particles are accelerated to 28–29 MeV. However, only a limited number of cyclotrons are capable of generating α-beam energies beyond 25 MeV [22]. A new high energy (30–70 MeV) cyclotron has been built in France which can produce $^{211}$At which could make the radionuclide more readily available, although its short $t_{1/2}$p (7 h) would still limit widespread distribution [23]. Another major limitation of α-emitters particularly for radiometals has been the chemistry for radiolabeling mAbs using bifunctional chelators. If α-decay yields daughter products that are α-emitters, the recoil energy released during α-decay can disrupt complexation of the radionuclide to the mAb (Fig. 6; discussed in Section 2.4). In most cases, the $t_{1/2}$p of the radionuclide should align with the pharmacokinetics of tumor uptake of the RICs. For solid tumors in which tumor accumulation is relatively slow, α-emitters with short $t_{1/2}$p (e.g. $^{213}$Bi; $t_{1/2}$p = 46 min or $^{211}$At; $t_{1/2}$p = 7 h) would be most suitable for labeling F(ab′)$_2$ fragments that are taken up by tumors and cleared more quickly from the blood [24], whereas for IgG forms, longer-lived α-emitters (e.g. $^{225}$Ac; $t_{1/2}$p = 10 days) may be more practical. However, there are exceptions in clinical scenarios in which the radiolabeled mAbs localize rapidly at sites of disease, e.g. targeting leukemic cells in the BM which occurs in minutes following intravenous (i.v.) administration of the radiolabeled mAbs. In these cases, short $t_{1/2}$p radionuclides could be feasible even for intact IgG forms of mAbs. Another consideration is that the radiation dose rate delivered to tumors is inversely proportional to the $t_{1/2}$p, with shorter-lived radionuclides delivering a higher dose. A higher dose rate would limit DNA repair and potentially maximize cytotoxicity to tumor cells.

In some cases, a radionuclide generator system may be used to produce short-lived daughter α-emitters from a longer-lived parent radionuclide. One example of such a generator system is the production of $^{212}$Bi ($t_{1/2}$p = 61 min) from $^{212}$Pb ($t_{1/2}$p = 10.6 days). $^{212}$Pb is produced by the decay of $^{224}$Ra to $^{220}$Rn, then to $^{216}$Po and then to $^{212}$Pb (Fig. 5A). Another example is the production of $^{213}$Bi ($t_{1/2}$p = 46 min) from the decay of $^{225}$Ac ($t_{1/2}$p = 10 days). $^{225}$Ac decays to $^{221}$Fr, then to $^{217}$At and finally to $^{213}$Bi (Fig. 5B). These generator systems have also been extended to in vivo production of radionuclides for RIT by labeling mAbs with the longer-lived $^{225}$Ac parent which decays to several shorter-lived daughter α- and β-emitters (Fig. 5A and B) [11]. However, as mentioned, the recoil energy released during α-decay combined with the different chemistry of these daughter products, results in instability of the RICs with possible release and redistribution of daughter radionuclides, potentially causing normal tissue toxicity [12].

### 2.4. Radiochemistry for labeling antibodies with α-emitters

Radiolabeling of mAbs with α-particle emitters that are radiometals usually relies on chelation by diethylenetriaminepentaacetic acid (DTPA) or 1,4,7,10-tetraazacyclododecane-1,4,7,10-tetraacetic acid (DOTA) (Table 1). Some novel chelators have been developed that provide faster and more stable complexation of the parent and daughter

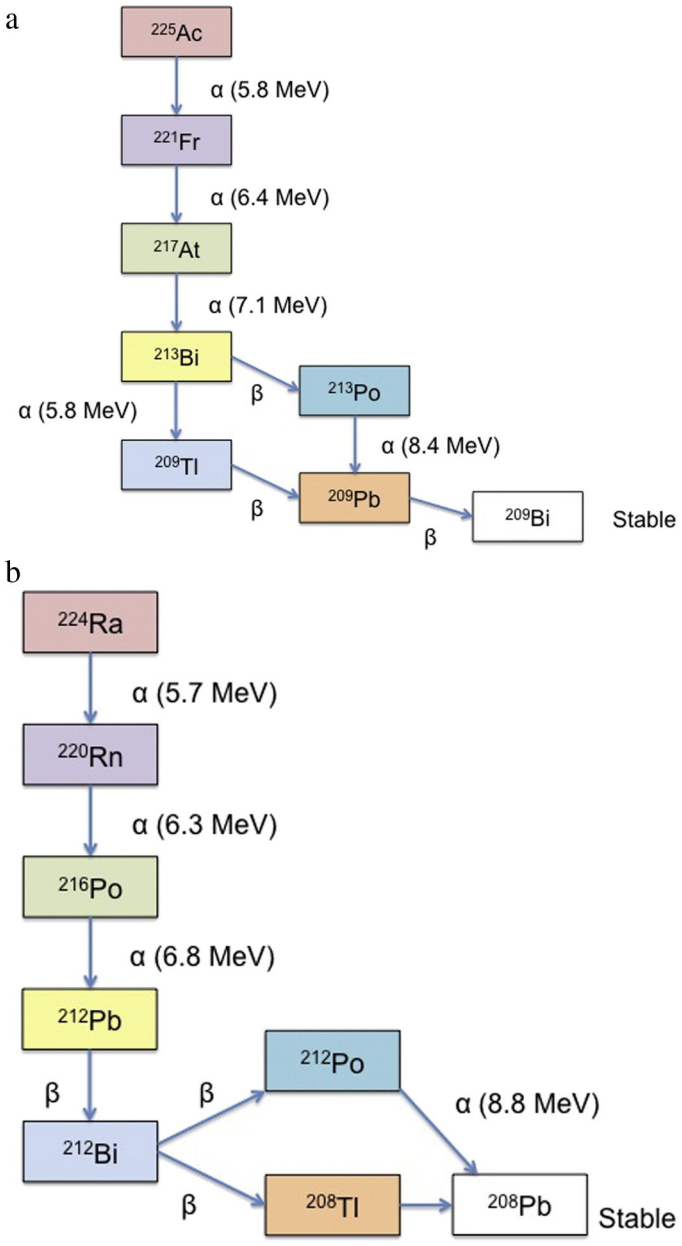


**Fig. 5.** Decay scheme of two α-emitting radionuclides ($^{224}$Ra and $^{225}$Ac) which decay to daughter radionuclides that are either α-particle emitters or β-particle emitters. The decay of a longer-lived parent radionuclide to shorter-lived daughter radionuclides is known as a radionuclide generator system. (A) $^{225}$Ac has been conjugated to monoclonal antibodies to provide an in vivo generator system for radioimmunotherapy that exploits the α-particle and β-particle emissions of $^{225}$Ac and its daughter products, including $^{213}$Bi (i.e. "atomic nanogenerator"). (B) $^{212}$Bi studied for radioimmunotherapy is produced through the decay of $^{212}$Pb, which is a daughter product in the decay scheme of $^{224}$Ra.

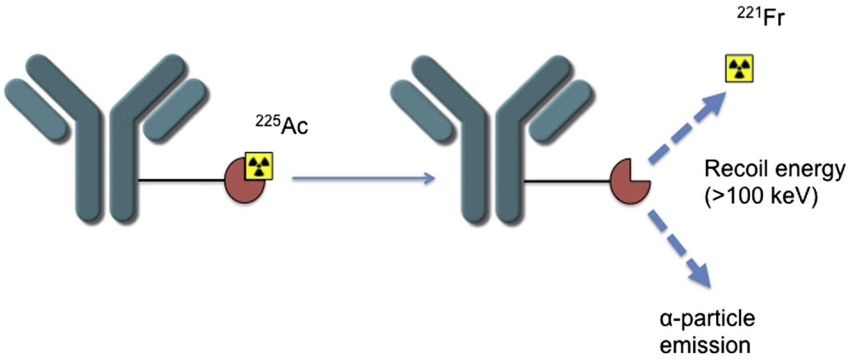


**Fig. 6.** The recoil energy released during α-particle decay combined with conversion of the parent radionuclide to a daughter radionuclide with different chelation chemistry results in release of radioactivity from the monoclonal antibody which may redistribute to normal tissues, potentially causing toxicity. The example shown is for a monoclonal antibody labeled with $^{225}$Ac which decays to $^{221}$Fr by release of an α-particle.

Please cite this article as: S. Aghevlian, et al., Radioimmunotherapy of cancer with high linear energy transfer (LET) radiation delivered by radionuclides emitting α-particles or ..., Adv. Drug Deliv. Rev. (2015), http://dx.doi.org/10.1016/j.addr.2015.12.003

**Table 1**
α-Particle emitters for conjugation to monoclonal antibodies for RIT of cancer.

| Radionuclide | Production method | α-Particle energy (MeV) | Physical half-life ($t_{1/2}$p) | Method for radiolabeling[a] |
|---|---|---|---|---|
| $^{225}$Ac | $^{223}$U → $^{225}$Ac | 5.8 | 10 days | Chelation by DOTA or NETA |
| $^{211}$At | $^{209}$Bi(α,2n)$^{211}$At | 7.4 | 7.2 h | Radioastatination |
| $^{212}$Bi | $^{212}$Pb → $^{212}$Bi | 6.0 | 61 min | Chelation by DTPA or DOTA |
| $^{213}$Bi | $^{225}$Ac → $^{213}$Bi | 6–8.4 | 46 min | Chelation by DTPA or DOTA |
| $^{212}$Pb | $^{224}$Ra → $^{212}$Pb | 6.0[b] | 10.6 h | Chelation by TCMC |
| $^{227}$Th | $^{227}$Ac → $^{227}$Th | 5.9 | 18.7 days | Chelation by DOTA |

[a] DOTA: 1,4,7,10-tetraazacyclododecane-1,4,7,10-tetraacetic acid; DTPA: diethylenetriaminepentaacetic acid; NETA: 4-[2-(bis-carboxymethyl-amino)-ethyl]-7-carboxymethyl-[1,4,7]triazonan-1-yl-acetic acid; TCMC: 2-(4-isothiocyanatobenzyl)-1,4,7,10-tetraaza-1, 4, 7, 10-tetra-(2-carbamoyl methyl)-cyclododecane.
[b] 212Pb decays by β-particle emission to 212Bi which emits an β-particle of this energy.

radionuclides. For example, the Bi(III) α-emitters, $^{212}$Bi and $^{213}$Bi, were studied via a Bi(III) surrogate, $^{205/206}$Bi, complexed to lintuzumab by *trans*-cyclohexyl DTPA (CHX-A-DTPA) which resulted in kidney accumulation of 10% injected dose/g (% ID/g) at 4 h post-injection [25]. In another study that compared several DTPA derivatives including CHX-A, and CHX-B (*cis*-cyclohexyl DTPA) conjugated to mAb B72.3 for complexing $^{206}$Bi, kidney uptake in mice ranged from 13.2–27.2% ID/g at 6 h post-injection [26]. Both the CHX-A and CHX-B $^{206}$Bi-immunoconjugates exhibited lower renal accumulation (9.3 and 7.8% ID/g), respectively [26]. These findings were confirmed in another study which reported 10-fold greater kidney uptake of radioactivity for $^{205}$Bi/$^{206}$Bi-DTPA-bevacizumab up to 4 h post-injection compared with $^{205}$Bi/$^{206}$Bi-CHX-A-DTPA-bevacizumab [27]. These studies demonstrated that CHX-A was a superior bifunctional chelator for complexing bismuth radionuclides. A novel octadentate chelator 4-[2-(bis-carboxymethyl-amino)-ethyl]-7-carboxymethyl-[1,4,7]triazonan-1-yl-acetic acid (NETA) has shown promise in further improving the biodistribution profiles of Bi(III)-labeled mAbs. $^{205/206}$Bi-NETA-trastuzumab exhibited a renal accumulation of 8% ID/g at 6 h post-injection, similar to the uptake of $^{205}$Bi/$^{206}$Bi complexed to CHX chelators [28]. A recent study presented in abstract form compared five different chelators for complexing $^{225}$Ac to the HER2 mAb, trastuzumab and the EGFR mAb, panitumumab [29]. NETA stably complexed both $^{225}$Ac and the daughter radionuclides $^{221}$Fr and $^{213}$Bi, indicating that the use of bifunctional chelators may provide a means to overcome the recoil energy of α-decay. $^{211}$At is a radiohalogen that normally requires astatination for radiolabeling mAbs, but a novel chelation method has been developed to complex $^{211}$At via an astatinated rhodium (III) complex stabilized with a tetrathioether macrocyclic ligand Rh[16aneS(4)-diol] [30].

The recoil energy (>100 keV) released during α-particle decay greatly exceeds the energy of a chemical bond [31] and combined with the different chemical properties of the daughter radionuclide may disrupt the linkage chemistry between the α-emitter and the mAb (Fig. 6) [32]. A study evaluating $^{225}$Ac-labeled anti-CD33 mAb, lintuzumab for treatment of leukemia engrafted into mice found that most of the radiation absorbed dose deposited in the kidneys was due to free $^{213}$Bi released from these RICs following α-particle decay of $^{225}$Ac [13]. Recently, this group showed that DOTA-lintuzumab constructs conjugated through a benzyl isothiocyanate side-chain on the chelator had more favorable radiolabeling kinetics than those conjugated through a N-hydroxysuccinimide linkage, and both constructs produced a therapeutic effect in NOD-scid gamma (NSG) mice inoculated i.v. with SET-2 leukemic cancer cells [33]. Another strategy to minimize the potentially harmful effects of released $^{213}$Bi, is the use of metal scavengers to sequester these radionuclides. For example, the oral metal chelator 2,3-dimercapto-1-propanesulfonic acid (DMPS) administered prior to injection of $^{225}$Ac-DOTA-lintuzumab significantly reduced the renal accumulation of $^{213}$Bi in mice and monkeys, but these protective effects were not seen with $^{221}$Fr, another daughter product of $^{225}$Ac (Fig. 5A) [32]. The authors also studied the use of diuretics to promote renal excretion of daughter radionuclides from decay of $^{225}$Ac. In biodistribution studies, administration of furosemide or chlorothiazide resulted in a significant reduction in kidney uptake in mice of $^{213}$Bi and $^{221}$Fr, at 24 h post-injection of $^{225}$Ac-DOTA-lintuzumab [32]. Finally, another strategy to overcome the instability of RICs emitting α-particles is local administration in close proximity to tumor cells, thereby decreasing the opportunity for redistribution of daughter products to normal tissues within the lifetime of the radionuclide. Local administration is feasible for treating intraperitoneal (i.p.) tumors by employing i.p. injection of the RICs and indeed, Phase I clinical trials have shown promise for this approach using $^{212}$Pb-labeled trastuzumab for treating HER2+ i.p. tumors (ClinicalTrials.gov Identifier: NCT01384253) [34,35]. The RICs in these studies employed 2-(4-isothiocyanotobenzyl)-1,4,7,10-tetraaza-1,4,7,10-tetra-(2-carbamoyl methyl)-cyclododecane (TCMC) to stably chelate $^{212}$Pb. Local instillation of $^{211}$At-labeled chimeric anti-tenascin C monoclonal antibody 81C6 into the surgical resection cavity in patients with glioblastoma multiforme (GBM), a type of brain malignancy, has also shown promising results [36].

### 2.5. Radioimmunotherapy studies with α-particle emitters

#### 2.5.1. $^{225}$Ac-labeled antibodies

The α-emitter $^{225}$Ac has a decay scheme that results in four daughter α-emitters as well as three β-particle emitters (Fig. 5A), making it an appealing radionuclide for RIT due to the radiation amplification effects. The Scheinberg group investigated RIT with $^{225}$Ac-labeled mAbs directed against several targets. They first coined the term *atomic nanogenerators* in 2001 to describe $^{225}$Ac-labeled RICs for treatment of mice with subcutaneous (s.c.) prostate cancer xenografts or disseminated human lymphomas [11]. These studies showed that a single dose of $^{225}$Ac-J591 (7.8 kBq) which targets prostate specific membrane antigen (PSMA), in mice bearing LNCaP prostate cancer tumors significantly extended median survival to 158 days compared to untreated mice which had a median survival of 33 days [11]. Also in this study, Daudi lymphoma cells were inoculated i.v. into mice to establish a disseminated cancer model. These mice were treated one day post-inoculation of Daudi cells with increasing doses of $^{225}$Ac-anti-CD19 B4 mAbs (2.1, 4.3 or 6.3 kBq) which resulted in prolonged survival to 99, 137 and 165 days, respectively, compared to mice treated with irrelevant $^{225}$Ac-lintuzumab (1.9 or 5.6 kBq) for which the survival was 36 and 43 days, respectively [11]. In a separate study, this group described treatment of HER2-positive SKOV-3 human ovarian cancer tumors in the peritoneal cavity of athymic mice following i.p. injected $^{225}$Ac-trastuzumab [37]. Dose-dependent increased survival was achieved using different dosing schedules and doses, with maximum median survival of 126 days obtained for 8.3 kBq $^{225}$Ac-trastuzumab given on day 1 and 14, compared to 48 days for irrelevant $^{225}$Ac-lintuzumab administered at the same dose and schedule, and 33 days for untreated mice [37]. This group also studied $^{225}$Ac-3F8 mAbs directed against ganglioside GD2 expressed in neuroblastoma [38]. Nude rats with NMB7 neuroblastoma meningeal carcinomatosis treated with $^{225}$Ac-3F8 achieved a median survival of 34 days compared to 18 days for rats treated with unlabeled 3F8 and 16 days for rats treated with control $^{225}$Ac-non-specific IgG or no treatment [38]. In a different approach, $^{225}$Ac-labeled E4G10, a mAb that binds to vascular endothelial cadherin on the tumor vasculature was studied for treatment of LNCaP prostate

Please cite this article as: S. Aghevlian, et al., Radioimmunotherapy of cancer with high linear energy transfer (LET) radiation delivered by radionuclides emitting α-particles or ..., Adv. Drug Deliv. Rev. (2015), http://dx.doi.org/10.1016/j.addr.2015.12.003

cancer xenografts in athymic mice [38]. RIT decreased tumor volume by 10-fold at 45 days post-treatment compared to untreated control mice or mice receiving unlabeled EG410 [38]. In mice with s.c. LS174T human colon cancer xenografts, RIT with $^{225}$Ac-E4G10 (2.2 kBq) combined with subsequent chemotherapy with leucovorin and 5-fluorouracil (5-FU) prolonged survival to 42 days, compared to the reverse order of treatment (chemotherapy followed by RIT) which increased survival to 26 days [39]. In a metastatic spontaneous mammary carcinoma mouse model, RIT with $^{225}$Ac-anti rat HER2 mAb 7.16.4, completely eradicated lung metastases in 67% of mice, and prolonged survival up to one year, compared to treatment with $^{213}$Bi-labeled or $^{90}$Y-labeled anti rat HER2 mAbs which provided median survivals of 61 and 50 days, respectively [9]. This study demonstrates the potential benefit of employing an in vivo nanogenerator ($^{225}$Ac) system for cancer treatment.

A clinical trial of RIT in patients with advanced myeloid leukemias with $^{225}$Ac-labeled lintuzumab has been completed but the results have not yet been published (ClinicalTrials.gov Identifier: NCT00672165). Another trial is investigating treatment with $^{225}$Ac-lintuzumab, following chemotherapy with low dose cytarabine to reduce the leukemic burden in patients with acute myeloid leukemia (AML). The goal of the Phase I component is to determine the MTD and the objective of the Phase II study is to determine if RIT administered at the MTD is effective for treatment of AML (ClinicalTrials.gov Identifier: NCT01756677). Early results presented at the American Society of Clinical Oncology (ASCO) annual meeting in June, 2015 indicated that the MTD had not yet been reached, but fractionated doses of $^{225}$Ac-lintuzumab (18.5, 37, or 55.5 kBq/kg/fraction for up to 4 cycles) provided objective responses in 3/12 patients [14].

#### 2.5.2. $^{211}$At-labeled antibodies

The limited availability of $^{211}$At remains an obstacle to the clinical use of this α-emitter, as it can only be produced by a cyclotron with sufficient energy, at least 28 MeV [40]. $^{211}$At availability is further restricted by the specialized methods required for isolation from the bismuth target in which the set-up, design, and dimensions of the target all affect the yield of $^{211}$At separation [40]. Nonetheless, the therapeutic potential of $^{211}$At-labeled mAbs in preclinical mouse models of metastatic ovarian cancer has been widely studied [41–45]. In these studies, mice were inoculated i.p. with ovarian cancer cells to establish a peritoneal carcinomatosis model. In one study, i.p. injection of $^{211}$At-labeled trastuzumab (400 kBq) eradicated i.p. HER2-positive SKOV-3 human ovarian cancer tumors [41]. Another study investigated the effectiveness of i.p. administered $^{211}$At-MX35 recognizing sodium-dependent phosphate transport protein 2b (NaPi2b) compared to non-specific $^{211}$At-labeled anti-CD20 mAb rituximab for RIT of i.p. OVCAR-3 ovarian cancer tumors in mice. These studies revealed that microscopic tumors (<30 μm in diameter) were effectively treated by $^{211}$At-MX35 and $^{211}$At-rituximab but when tumors reached a macroscopic size (>30 μm in diameter) only the specifically targeted $^{211}$At-MX35 RICs exhibited a therapeutic effect [42]. In a separate study, this group found that there was no significant advantage to administering $^{211}$At-MX35 in a fractionated regimen of three doses (267 kBq each) compared to one single dose (800 kBq), with 41% and 56% of mice becoming tumor-free [43]. Studies have similarly shown the effectiveness of $^{211}$At-MOv18 targeting folate receptors for RIT of mice engrafted i.p. with OVCAR-3 tumors following i.p. injection of RICs [46–48]. $^{211}$At-labeled mAbs have also proven effective for RIT in other tumor xenograft mouse models. These include $^{211}$At-ch81C6, which targets tenascin-C which was studied for RIT of s.c. human glioma xenografts [49], $^{211}$At-anti-Lewis Y mAbs studied for treatment of s.c. human colon cancer xenografts [50] and $^{211}$At-labeled 30F11 anti murine CD45 mAbs for treatment of AML in a syngeneic mouse leukemia model [51].

Promising results were obtained in a Phase I trial of $^{211}$At-ch81C6 for RIT of malignant gliomas which revealed low toxicity in patients with none experiencing dose-limiting toxicity [36]. The MTD was not reached. Phase I studies of $^{211}$At-MX35 F(ab′)$_2$ fragments administered i.p. to ovarian cancer patients deposited a potentially therapeutic radiation absorbed dose in microscopic tumor clusters without normal organ toxicity when treatment was combined with potassium perchlorate to block thyroid uptake of $^{211}$At released from the RICs [21].

#### 2.5.3. $^{212}$Bi-labeled antibodies

Preclinical studies with $^{212}$Bi-labeled anti-Tac mAbs have proven effective for RIT of interleukin-2 receptor (IL-2R)-positive T-cell leukemias [52,53]. $^{212}$Bi-anti-Tac mAbs injected i.p. also prolonged the survival of mice bearing s.c or peritoneal lymphoma xenografts [53]. One study investigated RIT with humanized $^{212}$Bi-anti-Tac mAbs in a murine plasmocytoma model in mice with i.p. or s.c. tumors [53]. $^{212}$Bi-anti-Tac (5.6–7.4 MBq) administered i.p. 3 days after i.p. inoculation of tumor cells prevented tumor formation in 75% of mice, whereas i.v. injection of $^{212}$Bi-anti-Tac inhibited tumor growth in about 30% of mice with s.c. tumors. The lower effectiveness of $^{212}$Bi-anti-Tac for treating s.c. tumors after i.v. injection was likely due to the very short $t_{1/2}$p (1 h) of $^{212}$Bi which limited the time available for tumor targeting of the RICs. In contrast, locoregional (i.p.) administration provided more rapid exposure of tumors in the peritoneal cavity. In another study, $^{212}$Bi-labeled 103A mAbs recognizing the viral Rauscher leukemia virus (RLV) glycoprotein gp70 prolonged the survival of mice with RLV-induced leukemia compared to $^{212}$Bi-labeled non-specific IgG or untreated mice [54]. No clinical trials have been reported for RIT using mAbs directly labeled with $^{212}$Bi, but human studies have been performed using $^{212}$Pb-labeled mAbs (see Section 2.5.4). $^{212}$Pb decays to $^{212}$Bi (Fig. 5B).

#### 2.5.4. $^{212}$Pb-labeled antibodies

Since $^{212}$Pb ($t_{1/2}$p = 10.6 h) decays to $^{212}$Bi ($t_{1/2}$p = 1 h), $^{212}$Pb-labeled immunoconjugates have been studied as in vivo generators of $^{212}$Bi, to prolong the exposure of tumors to $^{212}$Bi [6]. Several of these studies have focused on $^{212}$Pb-labeled trastuzumab (anti-HER2) or anti-EGFR cetuximab for RIT of disseminated i.p. LS174T human colon cancer tumors in mice [55–57]. In these studies, RIT was administered i.p. at 3-5 days after tumor cell inoculation when microscopic tumors were established. In one study, treatment of mice with i.p. tumors with the MTD of $^{212}$Pb-trastuzumab (0.37 MBq) prolonged survival by 3-fold compared to control mice treated with normal saline (56 days vs. 19 days, respectively) [55]. In another study using the same tumor xenograft mouse model, mice received one or two cycles of treatment with i.p. administration of 50 mg/kg gemcitabine (1 mg), a radiosensitizer, given 24 h before $^{212}$Pb-trastuzumab (0.37 MBq), then 0, 1, or 2 doses given at 1 week intervals. This RIT protocol further improved the effectiveness of RIT [56]. In this study the greatest effect was observed for mice that received two cycles of gemcitabine followed by RIT, then one subsequent gemcitabine injection 1 week later, resulting in a median survival of 197 days vs. 90 days for the same dosing schedule with only pre-treatment with gemcitabine, and 93 days for this schedule including two subsequent doses of gemcitabine following RIT [56]. This study demonstrates the importance of determining the optimal dosing regimen when combining RIT with radiosensitizing chemotherapeutic agents. Additionally, it is likely that these dosing regimens will need to be optimized for each radionuclide and antibody combination [58]. In another report, the chemotherapeutic agent paclitaxel (600 μg administered i.p.) enhanced the effects of RIT with $^{212}$Pb-trastuzumab (0.37 MBq) when injected 24 h prior to the RICs [59]. This combination treatment prolonged the median survival of tumor-bearing mice up to 171 days vs. 44 days for $^{212}$Pb-trastuzumab alone. Carboplatin administered i.p (1.25 mg) 24 h prior to RIT similarly improved survival to 157 days vs. 58 days for $^{212}$Pb-trastuzumab (0.37 MBq) alone [60]. The effectiveness of RIT (0.37 MBq) with $^{212}$Pb-labeled anti-EGFR cetuximab, $^{212}$Pb-labeled anti-HER2 trastuzumab and $^{212}$Pb-non-specific IgG were compared in this mouse model with i.p. inoculation of LS174T human colon cancer cells [57]. The median survival was prolonged for mice treated with $^{212}$Pb-cetuximab (84 days) or $^{212}$Pb-trastuzumab (113 days) compared to $^{212}$Pb-non-specific IgG (34 days) [57]. This study also confirmed that the therapeutic

effect of $^{212}$Pb-cetuximab was enhanced by pretreatment with i.p. gemcitabine. This combination prolonged survival to 283 days vs. 174 days for $^{212}$Pb-cetuximab alone [57]. Interestingly, in contrast to the previous results which showed an enhancement in the effectiveness of RIT combining $^{212}$Pb-trastuzumab with carboplatin, no increase in median survival was noted for $^{212}$Pb-cetuximab plus carboplatin. $^{212}$Pb-trastuzumab has also been studied for treatment of PC-3MM2 orthotopic human prostate cancer tumors in mice [61]. No systemic toxicity was observed at doses up to 0.74 MBq, and a single treatment decreased tumor growth by 60–74% compared to mice treated with unlabeled trastuzumab or receiving no treatment.

A Phase I clinical trial (ClinicalTrials.gov Identifier: NCT01384253) which investigated $^{212}$Pb-trastuzumab for RIT of patients with i.p. HER2+ ovarian, pancreatic or colon tumors has been completed. Dose-escalation studies using 5 dosage levels (7.4, 9.6, 12.6, 16.3, and 21.1 MBq/m$^2$) revealed minimal toxicity of i.p. infused $^{212}$Pb-trastuzumab following i.v. treatment with unlabeled trastuzumab (4 mg/kg) [35]. Due to the possibility of recoil mediated release of free $^{212}$Pb from the RICs during α-particle decay which may cause normal tissue toxicity, the U.S. Food and Drug Administration (FDA) required preclinical toxicity studies of unconjugated $^{212}$Pb which showed that at doses ranging from 0.0925–1.85 MBq injected i.p or i.v in Balb/c mice there was no significant toxicity [62]. A Phase I trial was performed in 3 patients with HER2+ ovarian cancer to study the biodistribution, pharmacokinetics, and tolerance of i.p. $^{212}$Pb-trastuzumab [34]. Imaging and pharmacokinetics showed minimal redistribution of $^{212}$Pb-TCMC-trastuzumab outside of the peritoneal cavity, and there was no major normal tissue toxicity.

### 2.5.5. $^{213}$Bi-labeled antibodies

$^{213}$Bi-labeled anti-CD138 mAbs administered i.v. at a dose of 3.7 or 7.4 MBq prolonged the survival of mice with i.v. disseminated 5T33 myeloma cells to 300 days and 227 days, respectively, vs. 46 days for mice receiving no treatment and 65 days for irrelevant $^{213}$Bi-antibody (6H4) [63]. $^{213}$Bi-labeled cetuximab was effective for killing EGFR-overexpressing triple-negative breast cancer (TNBC) cells in vitro, particularly cells with defective DNA repair caused by mutation in the BRCA-1 gene [64]. $^{213}$Bi-labeled humanized, domain-deleted CC49 (HuCC49ΔCH2) mAbs recognizing the cell-surface mucin, tumor-associated glycoprotein-72 (TAG-72) were compared to HuCC49ΔCH2 labeled with the β-emitter, $^{131}$I for treatment of s.c. LS-174T human colon cancer xenografts in mice [65]. RIT with $^{213}$Bi-HuCC49ΔCH2 at doses up to 37.0 MBq permitted 43–57% of tumor-bearing mice to survive for 64 days, while only 10–15% of mice treated with these doses of $^{131}$I-HuCC49ΔCH2 survived to this end-point [65]. $^{213}$Bi-labeled anti-CD45 YAML568 mAbs were effective for killing chemoresistant and radiation-resistant leukemia cells in vitro [66]. $^{213}$Bi-anti-CD45 mAbs caused DNA damage and apoptosis in HL-60 leukemia cells despite DNA repair mechanisms that make these cells resistant to β-radiation, γ-radiation, or doxorubicin-mediated apoptosis and DNA damage. The effect of early treatment at 1 or 8 days after tumor cell inoculation with $^{213}$Bi-anti-D9 mAbs (1.85 MBq) administered i.p was studied in mice with i.p. HSC45-M2 human gastric carcinoma cells expressing a mutated form of E-cadherin (D9-E-cad) [67]. More than 90% of mice treated at 1 day after tumor cell inoculation survived for 300 days, whereas <30% that received RIT (1.85 MBq) at 8 days survived to this end-point. These results indicate that α-particle RIT is most effective for treating small volume disease. Similar findings were noted in a study of $^{213}$Bi-labeled anti-EGFR matuzumab mAbs for RIT of orthotopic human bladder carcinoma xenografts in athymic mice [68]. Treatment with $^{213}$Bi-matuzumab (0.9 MBq) by intravesical (intra-bladder) injection at 1 h, 7 days, or 14 days after inoculation of EJ28 tumor cells permitted survival up to 300 days in 90%, 80% or 40% of mice, respectively. Untreated mice or mice receiving unlabeled matuzumab exhibited a median survival of 41 days and 89 days, respectively. In a subsequent study, fractionated doses of $^{213}$Bi-matuzumab, either two doses of 0.9 MBq (delivered on the first day of tumor detection and again at 7 days later) or three doses of 0.5 MBq (delivered on the first day of tumor detection and again at 4 and 8 days later) were injected intravesically following visualization of bladder tumors by bioluminescence imaging [69]. The two dose schedule yielded a median survival of 142 days with one third of mice surviving more than 268 days. The three dose schedule provided a median survival of 132 days with 30% of mice surviving longer than 300 days. Untreated mice and mice receiving unlabeled matuzumab had median survivals of 65 and 58 days, respectively. No toxic effects on normal tissues were observed. Preclinical studies combining cisplatin and carboplatin with $^{213}$Bi-labeled trastuzumab for RIT of i.p. LS-174T human colon cancer xenografts in mice revealed enhancement of the effectiveness of α-particle RIT, analogous to the results previously reported for $^{212}$Pb-trastuzumab [60]. However, enhancement effects on the survival of tumor-bearing mice were found only when cisplatin was concurrently administered with RIT, while administration of cisplatin prior to RIT, or 24 h after RIT was antagonistic. Carboplatin was also effective in enhancing the effectiveness of RIT with $^{213}$Bi-trastuzumab but was better tolerated [60]. Paclitaxel improved the effectiveness of RIT combined with $^{213}$Bi-trastuzumab [59]. $^{213}$Bi-labeled mAb 595 targeting the mucin-1 (MUC-1) glycoprotein expressed in pancreatic cancer (PnCa) was studied for killing PnCa cells in vitro and for RIT of PnCa tumors in vivo in athymic mice [70]. Apoptosis was induced in vitro by $^{213}$Bi-mAb 595 in 70–90% of CFPAC-1, PANC-1, and CAPAN-1 PnCa cells which have high or moderate MUC-1 expression. RIT with $^{213}$Bi-mAb 595 at two days post s.c. inoculation of CFPAC-1, PANC-1, or CAPAN-1 pancreatic cancer cells arrested tumor growth following intratumoral injection of 1.85 MBq, while i.v. injection of doses ranging from 2.8 to 8.3 MBq inhibited tumor growth in a dose-dependent manner.

Based on the results of preclinical studies of $^{213}$Bi-labeled anti-CD33 lintuzumab mAbs which demonstrated its effectiveness for RIT of AML engrafted into mice [25], a Phase I trial was conducted in 18 patients [71]. Doses up to 37 MBq/kg were well tolerated. RICs accumulated at sites of leukemia in the BM, liver, and spleen visualized by γ-scintigraphy, without significant kidney uptake of radioactivity that would be expected for released $^{213}$Bi. More than 93% of patients achieved reductions in leukemic blasts in the blood and 78% of patients achieved reductions in BM blasts. A subsequent Phase I/II trial combined $^{213}$Bi-lintuzumab (18.5–46.3 MBq/kg) with cytarabine chemotherapy for RIT of patients with AML [72]. The MTD of $^{213}$Bi-lintuzumab combined with cytarabine (200 mg/m$^2$/d) for 5 days was 37 MBq/kg. Partial or complete remission was achieved in 24% of patients receiving the MTD of $^{213}$Bi-lintuzumab but no responses were noted for patients who received lower doses.

### 2.5.6. RIT with combinations of mAbs and other α-emitters

Heterogeneity in the expression of tumor-associated antigens is a challenge for RIT of cancer. To overcome this limitation, anti-HER2 $^{213}$Bi-trastuzumab was combined with anti-TAG-72 $^{213}$Bi-HuCC49ΔCH2 for treatment of i.p. LS-174T human colon cancer tumors in mice [73]. Mice treated with either $^{213}$Bi-trastuzumab or $^{213}$Bi-HuCC49ΔCH2 exhibited a median survival of 31 days or 34 days, respectively, whereas combining these two RICs concurrently greatly increased survival to 147 days. Sequential administration of the two RICs only modestly increased survival [73]. Similar results were obtained by combining $^{212}$Pb-trastuzumab (0.2 MBq) with $^{212}$Pb-cetuximab (0.2 MBq) which yielded a median survival in mice with i.p. LS-174T tumors of 219 days vs. 182 days for $^{212}$Pb-trastuzumab (0.4 MBq) and 147 days for $^{212}$Pb-cetuximab (0.4 MBq) [57].

$^{227}$Th is a long-lived α-emitter ($t_{1/2}p = 18.7$ days) which decays to several daughter α-particle and β-particle emitting radionuclides ($^{223}$Ra, $^{219}$Rn, $^{215}$Po, $^{211}$Pb, $^{211}$Bi and $^{207}$Tl) and to stable $^{207}$Pb. This radionuclide conjugated through DOTA to trastuzumab showed specific tumor growth inhibition in mice with HER2-positive SK-BR-3 human breast cancer xenografts with no major normal organ toxicity including to the BM [74]. Interestingly, a direct comparison of α-particle RIT using $^{227}$Th-trastuzumab with β-particle RIT using $^{177}$Lu-trastuzumab in this

same mouse tumor xenograft model revealed that 0.4–1 MBq/kg of $^{227}$Th-trastuzumab provided equivalent tumor growth inhibition and prolonged survival as 200 MBq/kg of $^{177}$Lu-labeled trastuzumab, demonstrating the higher potency of α-particle RIT [10].

## 3. Radioimmunotherapy with Auger electrons

### 3.1. Properties of Auger electrons

Auger electrons are very low energy (<25 keV) electrons emitted by radionuclides that decay by electron capture (EC) and/or internal conversion (IC), two processes that introduce vacancies into the inner electronic shells of the daughter atoms (Fig. 4). These electrons were first discovered by Pierre Auger in 1925 [75]. The vacancies created by EC are filled by electrons decaying from higher shells creating subsequent vacancies that move progressively towards the outer shells. These transitions are ultimately accompanied by the emission of either a characteristic X-ray or low-energy Auger or IC electron [76]. IC electrons differ from Auger electrons in that they are not associated with emission of an X-ray, but instead the difference in energy between two electronic shells is transferred to an outer shell electron which is ejected by the atom. On average 5 to 50 electrons of different energies are emitted following every EC and/or IC event and because of their low energies, these electrons have a subcellular, nanometer range (<0.5 μm). The ejection of Auger electrons transiently imparts a positive charge on the decaying atom and deposits highly localized energy surrounding the site of decay. Due to their very short path length, Auger electrons have high LET (4 to 26 keV/μm) which causes multiple lethal DNA DSBs in cancer cells, particularly if these electrons are released in close proximity to nuclear DNA [77].

### 3.2. Radiobiological effects of Auger electrons

Since most Auger electrons have only nanometer range, their lethal DNA damaging effects is dependent on the position of radionuclide decay relative to the DNA duplex [76]. The Auger electron emitters $^{123}$I, and $^{125}$I conjugated to iododeoxyuridine (IUdR) which is incorporated directly into DNA strongly decreased mammalian cell survival [78,79]. The mean lethal dose of radiation for $^{125}$I-IudR was 7-fold lower than X-radiation indicating a high RBE value for the Auger electrons emitted by $^{125}$I [78]. In contrast, no major enhancement of cytotoxic effects compared to low LET γ-radiation [i.e. RBE < 2] was found for the Auger electron-emitters, $^{51}$Cr, $^{67}$Ga, $^{75}$Se, $^{125}$I, or $^{201}$Tl localized in the cytoplasm [80–83], bound to the cell membrane [83,84] or located outside the cell. Decay of an Auger electron-emitter in close proximity to nuclear DNA is therefore required to achieve a high RBE and fully exploit the high LET of these electrons for killing cells [80–83]. Other studies have compared the cytotoxicity of $^{125}$I incorporated into DNA. These studies investigated $^{125}$I-intercalators of DNA, $^{125}$I-minor/major-groove binders of DNA, $^{125}$I-oligonucleotides that formed a triplex with double-stranded DNA or hybridized with DNA or bound directly to DNA as transcription factors (reviewed in [76]). Dosimetric estimates revealed that the decay of $^{125}$I near the DNA duplex leads to very high radiation absorbed dose deposition ($10^9$ cGy/decaying atom) in the immediate vicinity of the decay site, followed by a sharp 1000-fold decrease in dose (to $10^6$ cGy/decay) with increasing distance up to a few nanometers from the DNA duplex [78,80,85]. Decay of an Auger electron-emitting radionuclide near but not within the DNA duplex efficiently generates single-strand breaks (SSB) and DSBs which are caused indirectly by hydroxyl radical (•OH)-mediated ionizations [86,87].

Since the lethal DNA damaging effects of Auger electrons are dependent on their proximity to nuclear DNA, recent studies have exploited nuclear translocation sequence (NLS) peptides to efficiently route mAbs labeled with the Auger electron-emitter, $^{111}$In to the cell nucleus following receptor-mediated internalization by cancer cells [88–90]. These 13-mer peptides (CGYGPKKKRKVGG) harbor the NLS of SV-40 large T-antigen [underlined] which interacts with the importin-α/β machinery to transport the mAbs across the nuclear membrane [91]. However, it has been argued that since the cell membrane has a critical function in cell survival, the effects of Auger electrons emitted by membrane-bound radiolabeled mAbs also need to be considered [92]. Ionizing radiation generates ceramide-enriched membrane microdomains which recruit pro-apoptosis factors or interfere with the binding of growth factors and survival proteins that trigger apoptosis [93–96]. Furthermore, the need for internalization of mAbs for Auger electron RIT has been questioned by recent studies that compared the cytotoxicity of radioactivity in the nucleus, at the cell surface or in the cytoplasm of A431 eidermoid cancer cells or SK-OV-3 ovarian cancer cells. The cells were exposed to internalizing $^{125}$I-labeled anti-EGFR 225 or anti-HER2 trastuzumab mAbs or non-internalizing anti-carcinoembryonic antigen (CEA) 35A7 mAbs or $^{125}$I-labeled tat peptides, which penetrate cells and are transported to the cell nucleus [92]. Although nuclear $^{125}$I was the most cytotoxic due to the DNA damaging properties of the Auger electrons, targeting the cell membrane proved more effective for killing cells than $^{125}$I deposited in the cytoplasm [92].

Auger electrons do not have a "cross-fire" effect that could irradiate and kill cells that are not targeted by the radiolabeled mAbs [97]. This is an advantage for minimizing the non-specific radiotoxicity of RIT towards non-targeted normal cells, especially hematopoietic stem cells in the BM, which is dose-limiting for mAbs labeled with β-emitters [1]. However, Auger electron RIT requires efficient targeting to cancer cells in order to achieve a cytotoxic effect and this may be limited by poor penetration of radiolabeled mAbs into solid tumors [24]. Nonetheless, Auger electron-emitters exhibit a localized "bystander effect" which promotes the apoptosis of non-targeted tumor cells that are proximal to targeted cells [98–100]. The bystander effect may be either tumor growth-inhibitory or paradoxically has been found in some cases to be tumor growth-stimulatory. For example, in male Ncr nude mice, co-inoculation of unlabeled LS174T human colon cancer cells with $^{125}$I-labeled cells demonstrated significant tumor growth inhibition compared to inoculation of only unlabeled cells, whereas a mixture of unlabeled and $^{123}$I-labeled cells exhibited enhanced tumor growth compared to inoculation of only unlabeled cells [100]. Another study found that the clonogenic survival of cancer cells was decreased by exposure to medium from cells that bound $^{123}$I-labeled metaiodobenzylguanidine ($^{123}$I-mIBG), demonstrating a bystander effect possibly mediated by release of cell toxins from irradiated cells [101]. Finally, Auger electrons have a more localized "cross-dose" effect in which targeted cells irradiate neighboring cells, [102]. These cross-dose and bystander effects may contribute to the effectiveness of Auger RIT for treatment of cancer [102].

### 3.3. Selection of an Auger electron-emitter for RIT

Several Auger electron-emitting radionuclides are available for radiolabeling mAbs (Table 2). There are several important factors that should be considered in selecting a radionuclide for Auger electron RIT. These include; i) the energy of the emitted electrons, ii) the ratio of penetrating forms of radiation (e.g. X-rays and γ-photons) compared to non-penetrating Auger electrons (p/e ratio), iii) the $t_{1/2}$p of the radionuclide, and iv) the method for radiolabeling the mAb. Since higher energy Auger and IC electrons penetrate a longer distance than lower energy electrons, these contribute a cytotoxic effect from the cell surface without the need for internalization or nuclear translocation. They also have a greater cross-dose effect due to their longer range, permitting killing of neighboring non-targeted cells in close proximity to the decay site, potentially overcoming heterogeneity in tumor localization of the radiolabeled mAbs. Finally, a radionuclide with a greater average electron energy would generally deposit more energy in a tumor cell. This explains the greater cytotoxicity of mAbs labeled with $^{67}$Ga which has a total electron energy of 34.4 keV but low electron yield (5.0 electrons/decay; Table 2) resulting in a higher average electron energy compared to $^{111}$In or $^{125}$I, radionuclides which have total electron energies of

Please cite this article as: S. Aghevlian, et al., Radioimmunotherapy of cancer with high linear energy transfer (LET) radiation delivered by radionuclides emitting α-particles or ..., Adv. Drug Deliv. Rev. (2015), http://dx.doi.org/10.1016/j.addr.2015.12.003

**Table 2**
Auger electron emitters for conjugation to monoclonal antibodies for RIT of cancer.

| Radionuclide | Production method | Electron yield per decay | Total electron energy (keV) | γ-photon energy (keV) and abundance | Physical half-life ($t_{1/2}$p) | Method for radiolabeling[a] |
|---|---|---|---|---|---|---|
| $^{125}$I | $^{124}$Xe(n,γ)$^{125}$Xe → $^{125}$I | 25.8 | 19.4 | 36(7%) | 57 days | Radioiodination |
| $^{123}$I | $^{124}$Xe(n,2n)$^{123}$Cs ⟶ $^{123}$Xe ⟶ $^{123}$I or $^{124}$Xe(p,pn)$^{123}$Xe ⟶ $^{123}$I | 15.1 | 27.6 | 159(83%) | 13.2 h | Radioiodination |
| $^{111}$In | $^{112}$Cd(p,2n)$^{111}$In | 14.9 | 32.7 | 171 (90%); 245 (94%) | 2.8 days | Chelation by DTPA or DOTA |
| $^{67}$Ga | $^{68}$Zn(p,2n)$^{67}$Ga | 5.0 | 34.4 | 93 (36%); 185 (20%); 300 (16%) | 3.3 days | Chelation by DFO or DOTA |
| $^{99m}$Tc | $^{99}$Mo ⟶ $^{99m}$Tc | 5.1 | 16.3 | 140 (98%) | 6.0 h | Chelation by HYNIC or $N_2S_2$ chelators |
| $^{64}$Cu | $^{64}$Ni(p,n)$^{64}$Cu | 4.0 | 18.2 | 511 keV (19%)[b] | 12.7 h | Chelation by DOTA or NOTA |

[a] DTPA: diethylenetriaminepentaacetic acid; DOTA: 1,4,7,10-tetraazacyclododecane-1,4,7,10-tetraacetic acid; DFO: desferrioxamine; HYNIC: hydrazinenicotinamide; N2S2: diamide dimercaptide; NOTA: 1,4,7-triazacyclononane-N,N′,N″-triacetic acid.
[b] Energy of the two annihilation γ-photons resulting from $^{64}$Cu positron emission.

32.7 keV and 19.4 keV, but higher electron yield (14.9 and 15.1 electrons/decay, respectively) [103]. Penetrating forms of radiation emitted in addition to the Auger electrons, especially γ-photons are useful to assess the delivery of the radiolabeled mAbs to tumors and normal organs by single-photon emission computed tomography (SPECT) but these may contribute to normal organ toxicity, especially at the high doses of radioactivity required for effective RIT [104]. Nonetheless, peptide-targeted radiotherapy with $^{111}$In-pentetreotide was well tolerated in patients with neuroendocrine tumors [105]. Only lymphocytopenia was noted which was possibly due to targeting of somatostatin receptor positive B-cells.

The physical half-life ($t_{1/2}$p) of the radionuclide is also an important consideration since a shorter $t_{1/2}$p provides a higher dose rate which may be beneficial by limiting DNA repair. However, a longer $t_{1/2}$p may contribute to normal organ toxicity since the RICs may be catabolized with redistribution of released radionuclides to normal tissues. Furthermore, non-specific irradiation of the BM by circulating RICs is increased for long $t_{1/2}$p radionuclides. Ultimately, the $t_{1/2}$p of the radionuclide should be compatible with the pharmacokinetics of tumor uptake of the RICs and elimination from the blood. Longer-lived radionuclides (e.g. $^{125}$I, $^{111}$In or $^{67}$Ga) are suitable for labeling intact IgG forms of mAbs while shorter-lived radionuclides ($^{123}$I, $^{99m}$Tc or $^{64}$Cu) may be more feasible for labeling F(ab′)$_2$ fragments that are eliminated more rapidly from the blood. However, short-lived Auger electron-emitting radionuclides may be used with intact IgG forms for targeting micrometastatic disease in the BM since localization occurs rapidly following i.v. injection. All studies of Auger electron RIT to date have employed intact IgG, but F(ab′)$_2$ fragments have been used for RIT with β-emitters or α-emitters [43,106–108]. Smaller engineered antibody fragments (e.g. recombinant Fab or single chain Fv) that are eliminated very rapidly from the blood have been studied mainly in pre-targeting approaches to RIT in which a bispecific antibody fragment is administered first to target the tumor followed by the radionuclide bound to a small molecule that recognizes the antibody in a second step [109,110].

Finally, the radiolabeling chemistry for mAbs is important since radioiodination methods (e.g. $^{123}$I or $^{125}$I) yield a radioimmunoconjugate that is unstable in vivo while complexation of radiometals (e.g. $^{111}$In, $^{67}$Ga or $^{64}$Cu) by bifunctional chelators is much more stable. Residualizing methods have been developed to stably substitute radioiodine onto mAbs [111]. Bifunctional chelators such as diethylenetriaminepentaacetic acid (DTPA), 1,4,7,10-tetraazacyclododecane-1,4,7,10-tetraacetic acid (DOTA) or 1,4,7-triazacyclononane-1,4,7-triacetic acid (NOTA) stably complex Auger electron-emitting radiometals such as $^{111}$In, $^{67}$Ga or $^{64}$Cu (Table 2). Radiometal-labeled mAbs exhibit higher tumor uptake than radioiodinated mAbs, but they also have higher and more persistent accumulation in the liver, spleen and kidneys [112].

### 3.4. Molecular targets for Auger electron RIT

#### 3.4.1. Epidermal growth factor receptors (EGFR)

The EGFR is the first member of the human epidermal growth factor receptor family which also includes the HER2, HER3 and HER4 receptors [113]. Binding of EGF to the EGFR causes receptor homodimerization or heterodimerization with other EGFR family members and initiates mitogenic signaling pathways [114]. EGFR overexpression with density up to 100-fold higher than on most normal epithelial tissues (~$10^5$–$10^6$ receptors/cell vs. <$10^4$ receptors/cell) has been found in many types of cancer and is often correlated with a poor prognosis [115]. The EGFR is thus an attractive target for the development of novel cancer therapeutics including RIT. However, careful consideration must be given to evaluating the toxicity of the radiolabeled mAbs towards some normal tissues that display moderate levels of these receptors including the liver and kidneys [116]. Nonetheless, mAbs targeted to the EGFR have been introduced into clinical practice for cancer treatment [117]. With particular relevance to Auger electron RIT of cancer, the EGFR also functions in a non-canonical manner as a transcriptional activator of cyclin D1 and iNOS genes in cancer cells, and this function is enabled by a putative NLS (RRRHIVRKRTLLR) found in the transmembrane domain of the receptor [118]. Nuclear EGFR has been associated with a poor prognosis in lung cancer [119] and breast cancer [120]. We found that conjugation of $^{111}$In-labeled anti-EGFR nimotuzumab mAbs to 13-mer peptides (CGYGPKKKRKVGG) harboring the NLS of SV-40 large T-antigen (underlined) increased their nuclear uptake in MDA-MB-468 cells compared to unmodified $^{111}$In-nimotuzumab up to 6 h after exposure, but not at 24 h, when nuclear importation of both RICs was equivalent [88]. The nuclear importation of $^{111}$In-nimotuzumab without NLS modification at this later time point may be mediated by the NLS in the EGFR. Nonetheless, $^{111}$In-NLS-nimotuzumab caused a 2-fold increase in DNA DSBs compared to $^{111}$In-nimotuzumab assessed by immunofluorescence for γ-H2AX foci in the nucleus [121]. The density of γ-H2AX foci following exposure to these RICs was 3-fold to 6-fold higher than in untreated cells. The clonogenic survival of MDA-MB-468 cells was reduced to <3% by $^{111}$In-NLS-nimotuzumab, whereas $^{111}$In-nimotuzumab without NLS modification was 7-fold less effective. The density of EGFR expression was also important and $^{111}$In-NLS-nimotuzumab was less effective for killing MDA-MB-231 human breast cancer cells that have a 10-fold lower EGFR density ($10^5$ vs. $10^6$ EGFR/cell). Both $^{111}$In-NLS-nimotuzumab and $^{111}$In-nimotuzumab localized in s.c. MDA-MB-468 tumor xenografts in mice. We have recently found that two doses of $^{111}$In-nimotuzumab (15.5 MBq; 3 mg/kg) separated by two weeks strongly inhibited the growth of MDA-MB-468 tumors by 4-fold compared to mice treated with $^{111}$In-labeled irrelevant $^{111}$In-trastuzumab, unlabeled nimotuzumab or mice receiving no treatment (unpublished results). There was no apparent toxicity of $^{111}$In-nimotuzumab at these doses to normal tissues including the liver and kidneys.

Michel et al. reported that 97–100% of A431 squamous cell carcinoma cells were killed by exposure in vitro to $^{111}$In or $^{125}$I labeled anti-EGFR mAb 528 [103]. These cells display a high density of EGFR (~$2 \times 10^6$ receptors/cell) [122]. As discussed earlier, mAbs labeled with radiometals such as $^{111}$In exhibit greater stability than $^{125}$I-labeled mAbs resulting in higher tumor accumulation [112]. Athymic mice with s.c. A431 tumor xenografts treated with $^{111}$In-labeled mAb 225 [2.7 MBq/g of body weight] exhibited two-fold longer survival compared to mice treated with $^{111}$In-labeled non-specific mAbs or no

Please cite this article as: S. Aghevlian, et al., Radioimmunotherapy of cancer with high linear energy transfer (LET) radiation delivered by radionuclides emitting α-particles or ..., Adv. Drug Deliv. Rev. (2015), http://dx.doi.org/10.1016/j.addr.2015.12.003

treatment [123]. Bender et al. reported that $^{125}$I-labeled F(ab′)$_2$ fragments of anti-EGFR mAb 425 killed >99% of EGFR-positive U87MG glioblastoma cells exposed in vitro to these RICs [124]. In this same study, F(ab′)$_2$ fragments of mAb 425 labeled with $^{125}$I were more effective for treating s.c. U87MG tumor xenografts in mice than $^{131}$I-labeled F(ab′)$_2$ fragments. It was proposed that the greater potency of $^{125}$I-mAb 425F(ab′)$_2$ compared to $^{131}$I-labeled F(ab′)$_2$ may be due to the ability of Auger electrons to more efficiently cause lethal DNA damage than the β-particles emitted by $^{131}$I. In a large clinical trial in which 180 patients with EGFR-positive glioblastoma multiforme (GBM) or astrocytoma were treated with adjuvant RIT following tumor surgical resection, single or multiple (up to 3) doses of $^{125}$I-mAb 425 (1295–3330 MBq; total 1480–8288 MBq), prolonged the expected survival in this patient population, with a median survival of 4–150 months for those with GBM and 4–270 months for patients with astrocytomas [125].

We previously studied targeted Auger electron radiotherapy of EGFR-positive breast cancer using $^{111}$In-labeled human EGF ($^{111}$In-DTPA-hEGF), a peptide ligand for the receptor. Although not RIT, these studies provide insight into targeting EGFR with Auger electron-emitting radiopharmaceuticals. $^{111}$In-DTPA-hEGF was bound, internalized and translocated to the nucleus of EGFR-positive MDA-MB-468 human breast cancer cells (~$10^6$ EGFR/cell), and strongly inhibited the growth of these cells [126]. A subsequent study showed that >98% of MDA-MB-468 cells were killed by exposure in vitro to $^{111}$In-DTPA-hEGF. This decreased clonogenic survival was directly correlated with the density of DNA DSBs in the nucleus of these cells caused by the Auger electrons, assessed by immunofluorescence for γ-H2AX foci [127]. However, the cytotoxicity of $^{111}$In-DTPA-hEGF was dependent on EGFR density with lower potency observed for MDA-MB-231 or MCF-7 breast cancer cells that have moderate ($10^5$ EGFR/cell) or low ($10^4$ EGFR/cell) receptor expression, respectively [128]. $^{111}$In-DTPA-hEGF strongly inhibited the growth of MDA-MB-468 tumors in mice with no major effects on hematological function or increases in serum transaminases or creatinine that would indicate liver or kidney toxicity, respectively [129]. The lack of normal organ toxicity of $^{111}$In-DTPA-hEGF was confirmed in a comprehensive study that examined its effects on a panel of normal tissues as well as on hematological, liver and kidney function [116]. An important consideration in targeting EGFR with Auger electron-emitting agents is that since <3% of the hematopoietic stem cell population are EGFR-positive [130] and cellular binding and internalization are required for cytotoxicity from the Auger electrons, this greatly minimized the toxic effects of $^{111}$In-DTPA-hEGF on normal hematological function. A Phase I clinical trial in 16 patients with EGFR-positive metastatic breast cancer administered 357–2290 MBq (0.5 mg) of $^{111}$In-DTPA-hEGF similarly revealed no normal organ toxicity including to the liver and kidneys which have moderate EGFR expression [131]. However, some adverse effects (flushing, chills, nausea and vomiting and transient hypotension) related to the biological activity of EGF were noted. Tumor uptake of $^{111}$In-DTPA-hEGF was visualized by γ-scintigraphy in 7 of 15 evaluable patients, but no objective responses were found at the relatively low doses examined in the trial. A comparison of the tumor and normal tissue localization of $^{111}$In-DTPA-hEGF and $^{111}$In-labeled anti-EGFR mAb 528 in mice with s.c. MDA-MB-468 xenografts revealed 10-fold greater tumor uptake for $^{111}$In-labeled mAb 528 [21.6% injected dose/g (% ID/g) vs. 2.2% ID/g, respectively]. The higher tumor uptake of $^{111}$In-mAb 528 compared to $^{111}$In-DTPA-hEGF suggests that RIT could be more effective than peptide-targeted radiotherapy with Auger electrons. Moreover, anti-EGFR mAbs would be associated with fewer biologically-mediated side-effects than $^{111}$In-DTPA-hEGF, although the anti-EGFR mAb cetuximab is known to cause skin rashes associated with its binding to the EGFR that are predictive of a good response to this agent [132]. A truncated non-biologically-active form of EGF (EGFt) has recently been produced which retains EGFR binding, internalization and nuclear translocation [133] and may circumvent the EGF-mediated adverse effects found for $^{111}$In-DTPA-EGF. However, $^{111}$In-labeled EGFt was less efficient for delivery of $^{111}$In into EGFR-positive breast cancer cells and less potent for killing these cells in clonogenic assays [134].

### 3.4.2. Human epidermal growth factor receptor-2 (HER2)

HER2 is overexpressed in about 25% of cases of breast cancer, in most cases due to *HER2* gene amplification and is the target for immunotherapy with trastuzumab, pertuzumab and the antibody-drug immunoconjugate (ADC), trastuzumab-emtansine (T-DM1) [135]. HER2 is only slowly internalized compared to other EGFR family members [136] but harbors an NLS which routes internalized receptors to the nucleus [137]. Trastuzumab promotes internalization of HER2 which is one of the putative mechanisms of action of the drug [138,139]. Despite pre-selection of patients with tumors classified as HER2+ for treatment with trastuzumab combined with chemotherapy, only about 1 in 2 patients with metastatic HER2+ breast cancer benefit from this treatment regimen [140], and almost all patients develop resistance within a year [141]. RIT may be one strategy which could improve the response to trastuzumab and overcome tumor resistance.

Our group previously investigated Auger electron RIT targeting HER2 using $^{111}$In-trastuzumab modified with NLS peptides. $^{111}$In-NLS-trastuzumab was imported into the nucleus of human breast cancer cells following receptor-mediated internalization, in proportion to the HER2 density [90]. $^{111}$In-NLS-trastuzumab was 5-fold more cytotoxic in vitro to SK-BR-3 human breast cancer cells overexpressing HER2 ($10^6$ receptors/cell) than $^{111}$In-trastuzumab without NLS, killing >90% of cells in clonogenic assays, whereas unlabeled trastuzumab reduced the survival of these cells by only 1.5-fold (Fig. 7). Cell killing by $^{111}$In-NLS-trastuzumab was associated with a 4-fold increase in DNA DSBs assessed by probing for γ-H2AX foci in the nucleus compared to untreated cells. $^{111}$In-NLS-trastuzumab localized in s.c. HER2-positive MDA-MB-361 human breast cancer xenografts (12% ID/g at 72 h post-injection) and nuclear uptake in tumor cells measured ex vivo was 2.6-fold greater than $^{111}$In-trastuzumab without NLS modification. In a subsequent study, it was shown that the cytotoxic potency of $^{111}$In-NLS-trastuzumab against breast cancer cells in vitro was increased by up to 1.7-fold when combined with methotrexate, a chemotherapeutic agent that interferes with folate synthesis thus depleting the pool of nucleotides required for DNA repair [142]. Moreover, $^{111}$In-NLS-trastuzumab killed TrR1 human breast cancer cells that have acquired resistance to trastuzumab despite continued HER2 expression [143]. These results suggest that Auger electron RIT may be able to overcome resistance to trastuzumab in breast cancer. Similar radiosensitization of breast cancer cells to the effects of the $^{111}$In-NLS-trastuzumab were found for paclitaxel which interferes with microtubule formation, arresting the cells in the more radiation sensitive G2/M-phase of the cell cycle and for doxorubicin, which intercalates into DNA interfering with DNA synthesis required for strand break repair [144]. Treatment of mice with s.c. MDA-MB-361 tumors with a single dose of $^{111}$In-NLS-trastuzumab (9.25 MBq; 4 mg/kg), a level selected to cause no observable adverse effects (NOAEL) inhibited tumor growth by 4–5 fold compared to untreated mice (Fig. 7) [104]. $^{111}$In-NLS-trastuzumab was 2-fold more effective than $^{111}$In-trastuzumab and 3-fold more effective than unlabeled trastuzumab.

While the results with $^{111}$In-NLS-trastuzumab are encouraging, a limitation was the low specific activity (SA) obtained for these RICs (<0.24 MBq/μg) which resulted in only 1 in 50 trastuzumab molecules labeled with $^{111}$In, causing a high proportion of HER2 on breast cancer cells to be targeted by unlabeled immunoconjugates, limiting the cytotoxic potency. In order to increase the SA of the RICs, we have site-specifically conjugated onto the Fc domain of trastuzumab, a metal-chelating polymer (MCP) that presents multiple DTPA for complexing $^{111}$In. The MCP was composed of a polyglutamide backbone with 24 or 29 pendant DTPA groups with or without NLS peptide modification [145]. The maximum SA for labeling these MCP-trastuzumab immunoconjugates with $^{111}$In was increased by 90-fold (8.9 vs.

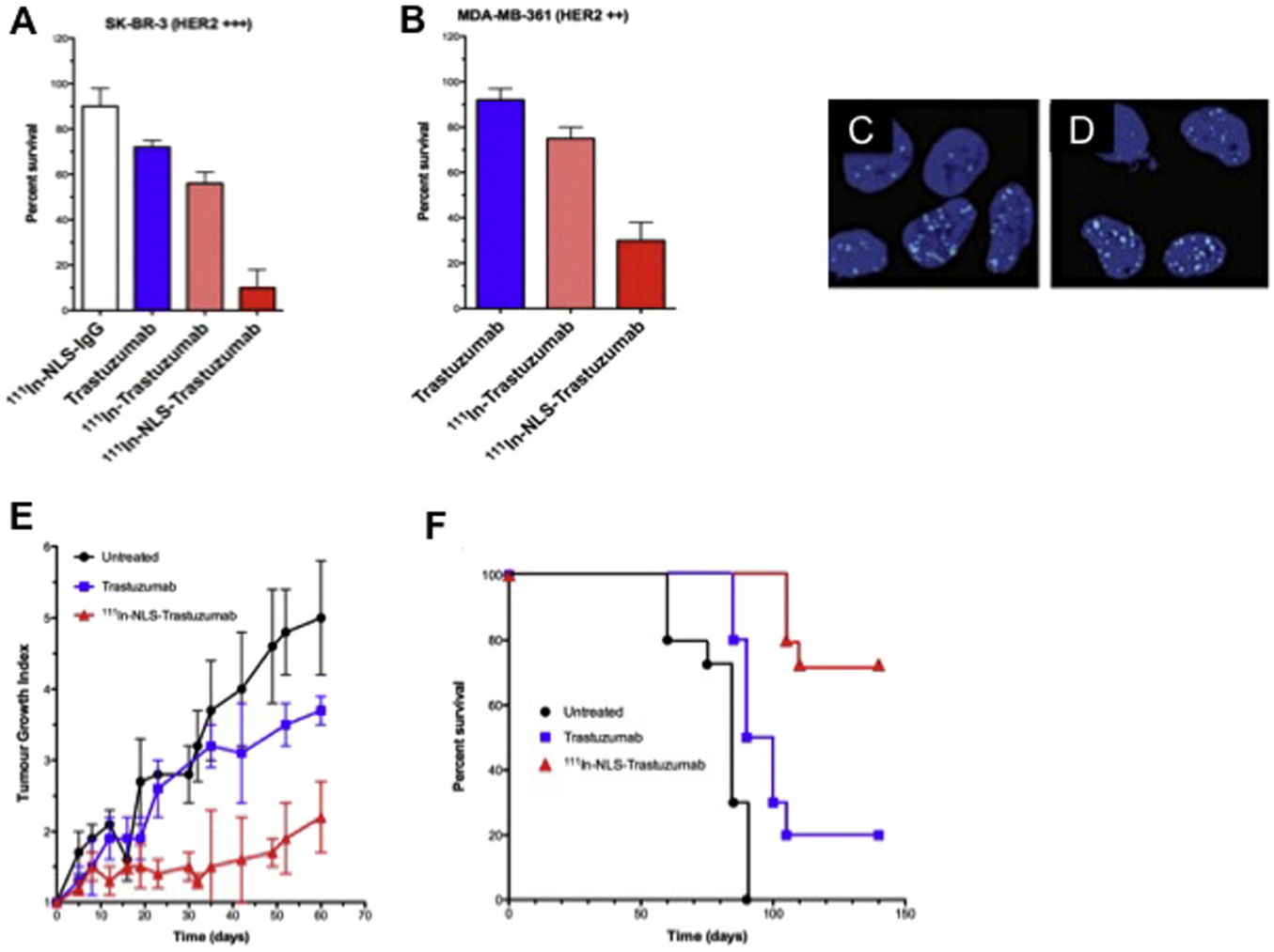


**Fig. 7.** Clonogenic survival of SK-BR-3 human breast cancer cells with high HER2 expression (A) or MDA-MB-361 cells with intermediate HER2 density (B) exposed in vitro to 70 μg/mL of non-specific $^{111}$In-NLS-IgG, unlabeled trastuzumab (Herceptin), $^{111}$In-trastuzumab or $^{111}$In-NLS-trastuzumab. DNA double-strand breaks in the nucleus of (C) SK-BR-3 or (D) MDA-MB-361 cells exposed in vitro to $^{111}$In-NLS-trastuzumab detected by immunofluorescence for γ-H2AX (bright foci). The nucleus is counterstained with DAPI (diaminobenzidine). (E) Tumor growth vs. time in mice with s.c. MDA-MB-361 xenografts following treatment with a single dose of $^{111}$In-NLS-trastuzumab (9.25 MBq, 4 mg/kg) or an equivalent mass dose of unlabeled trastuzumab (Herceptin) or no treatment. (F) Survival of mice with MDA-MB-361 tumors treated with two doses (9.25 MBq, 4 mg/kg) of $^{111}$In-NLS-trastuzumab or two single doses of unlabeled trastuzumab (Herceptin) separated by 14 days or receiving no treatment. Modified and adapted from D.L. Costantini et al. J. Nucl. Med. 48 (2007) 1357–68 and D.L. Costantini et al. J. Nucl. Med. 51 (2010) 1084–91.

0.1 MBq/μg, respectively) compared to trastuzumab substituted with only two DTPA groups [146]. Conjugation of trastuzumab to MCPs that harbored NLS peptides did not increase nuclear importation in HER2-positive SK-BR-3 cells. This could be explained by nuclear translocation of $^{111}$In-MCP-trastuzumab by the endogenous NLS in the HER2 receptor [137]. $^{111}$In-MCP-trastuzumab (5.5 MBq/μg) increased DNA DSBs by 6-fold in *HER2* gene amplified SK-BR-3 cells and killed >98% of these cells in clonogenic assays, whereas low SA $^{111}$In-DTPA-trastuzumab (0.37 MBq/μg) reduced cell survival by only 3-fold. Exposure to $^{111}$In-MCP-trastuzumab decreased the survival of Zr-75-1 cells which have intermediate HER2 density ($4 \times 10^5$ receptors/cell) but are not *HER2* gene amplified by 5-fold and trastuzumab-resistant TrR1 cells with intermediate HER2 density ($5 \times 10^5$ receptors/cell) by 6-fold. In contrast, unlabeled trastuzumab reduced the clonogenic survival of SK-BR-3 and Zr-75-1 cells by 2–3 fold and was ineffective for killing TrR1 cells [146]. Similarly increased cytotoxic potency against HER2 + breast cancer cells was observed for trastuzumab linked to G4 polyamidoamine (PAMAM) dendrimers functionalized with multiple DTPA chelators for labeling with $^{111}$In to high SA [147]. A novel strategy which employs a single platform to combine radiosensitizers and $^{111}$In for Auger electron RIT was reported by Hoang et al. who constructed block copolymer micelles (BCMs) modified with trastuzumab Fab fragments linked to NLS peptides and polymers derivatized with DTPA for complexing $^{111}$In, and methotrexate loaded into the core of the micelles [148]. $^{111}$In-labeled BCMs were specifically bound and internalized by HER2 + breast cancer cells and routed to the cell nucleus. These $^{111}$In-labeled micelles selectively killed SK-BR-3 or MDA-MB-361 cells overexpressing HER2.

The density of cell surface receptors is important for RIT since this limits the amount of radioactivity which can be delivered to a cancer cell at a given SA of the RICs. Targeting cancer cells with a mixture of radiolabeled mAbs recognizing different epitopes may be more effective than targeting a single population of receptors since it increases the total density of receptors available for RIT. Michel et al. demonstrated that exposure of HER2 + SK-BR-3 cells to a mixture of $^{111}$In-labeled mAbs 21.1 and 4D5 which bind to non-competing epitopes on HER2 almost completely eradicated these cells [149]. Radioresistant SK-OV-3.ip.1 human ovarian cancer cells were less effectively killed by radiolabeled mAbs targeting a single epitope but their survival was decreased to <0.2% by the combination of $^{111}$In-labeled 21.1 and 4D5. In a subsequent study, Mattes and Goldenberg treated mice at 5–6 days after s.c. inoculation of HER2 + SK-OV-3 ovarian cancer cells with 59 MBq of $^{111}$In-labeled 4D5 mAbs to study the effects of RIT on prevention of tumor growth and long-term survival. RIT delayed tumor growth and 4/11 mice were cured. RIT with $^{111}$In-labeled 4D5 prolonged survival

by 3.6-fold compared to control mice treated with $^{111}$In-labeled non-specific mAbs or receiving no treatment [123].

*3.4.3. Other targets on solid tumors for Auger electron RIT*

MAb A33 recognizes a cell-surface glycoprotein expressed on >95% of human colon cancers [150]. Barendswaard et al. reported that a 4.5-fold higher dose of $^{125}$I-labeled mAb A33 compared to $^{131}$I-A33 was required for equivalent tumor growth-inhibition in mice with s.c. SW1222 human colon cancer xenografts [151]. However, since the MTD of $^{125}$I-A33 was 10-fold higher than for $^{131}$I-A33, there was a 2-fold improvement in the therapeutic index for Auger electron RIT with $^{125}$I-A33 compared to β-particle RIT with $^{131}$I-A33. Others have similarly shown that mAbs labeled with Auger electron-emitters (e.g. $^{125}$I and $^{111}$In) are more effective for RIT of cancer than mAbs labeled with radionuclides emitting β-particles (e.g. $^{131}$I and $^{90}$Y) when administered at equitoxic doses [152,153]. In a Phase I/II clinical trial, 21 patients with chemotherapy-resistant metastatic colon cancer were treated with increasing doses of $^{125}$I-A33 up to 12,950 MBq/m$^2$ without any major normal tissue toxicities and the MTD was not reached [154]. Decreased serum carcinoembryonic antigen (CEA) levels were noted in 3/21 patients and an additional patient exhibited a mixed tumor response by CT imaging. Interestingly, a Phase I/II trial of $^{131}$I-labeled A33 in 20 patients with metastatic colon cancer revealed that the MTD was 2775 MB/m$^2$, which is almost 5-fold lower than for $^{125}$I-A33, demonstrating the higher safety margin for Auger electron RIT [155]. A similar rate of response was observed for RIT with $^{131}$I-A33, as CEA levels decreased in two patients and mixed tumor responses were detected on CT in three patients. CO17-1A mAb binds to GA733, a tumor-associated antigen highly expressed in colon cancer. Exposure of SW1116 colon cancer cells to $^{125}$I-labeled CO17-1A decreased the survival of these cells by more than 1000-fold and caused chromosomal damage [152]. The MTD for $^{125}$I-CO17-1A was 10-fold greater than $^{131}$I-CO17-1A in mice with s.c. GW-39 human colon cancer xenografts [152]. The MTD of $^{111}$In-labeled CO17-1A was 30-fold higher than for $^{90}$Y-labeled CO17-1A (4 MBq vs. 118 MBq, respectively). Nonetheless, myelosuppression remained dose-limiting for Auger electron RIT.

*3.4.4. Auger electron RIT of B-cell lymphomas*

The high abundance of the major histocompatibility complex class II (MHC) γ-chain (CD74) on B-cell lymphoma cells combined with the efficient internalization of anti-CD74 mAb LL1, makes CD74 an attractive target for Auger electron RIT [156,157]. Griffiths et al. reported that exposure to $^{125}$I-, $^{111}$In- or $^{99m}$Tc-labeled mAb LL1 killed 99–100% of Raji B-cell lymphoma cells [158]. The effectiveness of mAb LL1 labeled with $^{67}$Ga, $^{125}$I, or $^{111}$In or the β-emitters, $^{131}$I or $^{90}$Y for killing Raji cells in vitro was compared [159]. The order of effectiveness was: $^{131}$I > $^{67}$Ga > $^{90}$Y > $^{125}$I > $^{111}$In. The greater proportion of higher energy electrons emitted by $^{67}$Ga compared to $^{125}$I or $^{111}$In deposited more radiation in the nucleus from the cell membrane or cytoplasm, which rendered $^{67}$Ga-labeled LL1 more effective than $^{125}$I or $^{111}$In-labeled antibodies. However, Auger electron emitters showed greater specificity than the β-emitters, $^{131}$I or $^{90}$Y. Specificity was defined as the ratio of the concentration of LL1 compared to non-specific mAbs required for killing 99% of the cells. The effectiveness of $^{111}$In and $^{125}$I-LL1 for killing Ramos, RL and Daudi B-cell lymphoma cells in vitro was further demonstrated [160]. In a mouse model of disseminated Raji B-cell lymphoma, RIT with $^{67}$Ga-labeled LL1 (9 MBq) or $^{111}$In-LL1 (13 MBq) prevented tumor formation, whereas tumors were only minimally controlled by treatment with LL1 labeled with the β-emitter, $^{90}$Y administered at the MTD (0.9 MBq) [161]. These results are likely due to the subcellular range and high LET of Auger electrons, eradicating cells in the circulation and preventing tumor formation. However, in a subsequent study in mice implanted with s.c. Raji, Daudi or RL B-lymphoma xenografts, the growth of established macroscopic tumors were not well controlled by Auger electron RIT with 10.4 MBq $^{111}$In- or 8.7 MBq $^{125}$I-labeled anti-CD74 or anti-CD20 mAbs. The largest tumor that could be effectively treated was approximately 2 mm in diameter.

Michel et al. compared 1F5 and L243 mAbs that bind CD20 or the MHC class II α/β chain epitopes, respectively, labeled with the Auger electron-emitters, $^{67}$Ga, $^{125}$I, $^{111}$In, or $^{131}$I for killing Raji B-cell lymphoma cells [162]. The order of cytotoxicity was similar to that found previously for LL1 mAbs ($^{131}$I > $^{67}$Ga > $^{125}$I > $^{111}$In). $^{67}$Ga was 2–3 fold more effective than $^{111}$In which reflected its greater proportion of more energetic Auger and IC electrons. $^{131}$I-labeled mAbs non-specifically killed Raji cells but $^{111}$In-labeled mAbs also exhibited some non-specific cytotoxicity towards these cells at high concentrations. MAb 1F5 is internalized and translocated to the nucleus in Raji cells which is expected to enhance its effectiveness for Auger electron RIT [163]. However $^{111}$In-labeled mAb 1F5 (10.4 MBq) proved ineffective for preventing the formation of s.c. Raji tumors in 80% of mice, whereas this RIT agent was highly effective for treatment RL B-cell lymphoma xenografts that are more radiation sensitive than Raji cells [164]. These findings highlight the importance of tumor radiation sensitivity in assessing the outcome of RIT.

*3.4.5. Auger electron RIT of acute myeloid leukemia (AML)*

There is a critical need for novel treatments for AML, since only 1 in 4 patients diagnosed with this disease survive more than 5 years despite intensive chemotherapy in some cases combined with hematopoietic stem cell transplant [165]. CD33 is a 67 kDa cell-surface adhesion molecule that is expressed on 80–90% of AML cells as well as differentiated normal myeloid cells, but not on the earliest myeloid progenitor cells, which should spare these cells from the toxic effects of RIT [166]. Preclinical and clinical studies demonstrated that $^{131}$I-labeled murine M195 or humanized M195 (HuM195) anti-CD33 mAbs efficiently killed AML cells [167,168]. However, non-specific irradiation of the BM by the long-range (2 mm) β-particles emitted by $^{131}$I (cross-fire effect) causing myelosuppression remains a major challenge. To improve the selectivity of radiolabeled anti-CD33 mAbs for killing leukemic cells, we have studied Auger electron RIT of AML using $^{111}$In-labeled M195 or HuM195 mAbs modified with NLS peptides to route the RICs to the nucleus following CD33-mediated internalization [89]. HL-60 leukemia cells displaying CD33 were completely eradicated in vitro following exposure to $^{111}$In-NLS-HuM195. Furthermore, the clonogenic survival in vitro of primary leukemia specimens from AML patients was reduced up to 10-fold following exposure to $^{111}$In-NLS-HuM195. Moreover, in contrast to the myelosuppression found for $^{131}$I-HuM195 [168], there were no adverse effects on the hematopoietic system or on the liver or kidneys in mice injected with $^{111}$In-NLS-HuM195 at low doses up to 3.7 MBq. Interestingly, $^{111}$In-NLS-HuM195 was able to kill HL-60 MX-1 leukemia cells resistant to methotrexate chemotherapy and patient AML specimens that displayed multidrug resistance (MDR) transporters responsible for chemotherapy resistance, suggesting that Auger electron RIT may be able to overcome resistance to chemotherapy [169]. However, a limitation for $^{111}$In-NLS-HuM195 is the relatively low CD33 density (~4 × 10$^4$ receptors/cell) present on leukemia cells and the heterogeneity in CD33 expression between patient AML specimens requiring a minimum specific activity (SA) of 2–3 MBq/mg for effective cell killing [89,169].

AML is believed to be initiated by a malignant leukemic stem cell (LSC) that is derived from a normal hematopoietic stem cell, which populates downstream leukemic blasts in the BM and blood [170]. Recurrence of AML following intensive chemotherapy may be due to survival of the LSC subpopulation since these cells exhibit high expression of MDR transporters [171,172]. Strategies that target the LSC could provide more durable remissions, and potentially provide an opportunity for cure. A unique feature of LSCs is their overexpression of the interleukin-3 receptor α-subchain (CD123) relative to the β-subchain (CD131) [173]. Monoclonal antibody 7G3 and its chimeric analogue, CSL360 (CSL Ltd., Parkville, Australia) preferentially bind to leukemic cells that display the CD123$^+$/CD131$^-$ phenotype of the LSC subpopulation [174]. We have developed Auger electron RIT agents that target LSC by modifying mAb 7G3 or CSL360 with NLS peptides and DTPA for

Please cite this article as: S. Aghevlian, et al., Radioimmunotherapy of cancer with high linear energy transfer (LET) radiation delivered by radionuclides emitting α-particles or ..., Adv. Drug Deliv. Rev. (2015), http://dx.doi.org/10.1016/j.addr.2015.12.003

labeling with $^{111}$In [175,176]. MicroSPECT/CT imaging revealed that $^{111}$In-NLS-7G3 and $^{111}$In-NLS-CSL360 localized specifically at sites of leukemia engrafted into the BM and spleen of NOD/SCID mice using human AML cell lines or primary patient AML specimens [175,176]. Both $^{111}$In-NLS-7G3 and $^{111}$In-NLS-CSL360 were effective for reducing the clonogenic survival of AML cells sharing the CD123$^{+}$/CD131$^{-}$ phenotype of LSCs [175] and this cytotoxicity was amplified by co-exposing these cells to A12B4C3, an inhibitor of DNA repair [177]. Studies are now in progress to investigate these RIT agents for treatment of AML in NOD/SCID mice. Initial results revealed a decrease in CD123$^{+}$ leukemic cells, impairment of LSC self-renewal, and eradication of leukemia from the BM in some mice [178].

## 4. Conclusions

RIT is a promising and theoretically sound approach that has proven very effective for treatment of multiple tumor types in preclinical mouse tumor xenograft models and clinically in patients with non-Hodgkin's B-cell lymphoma. The major challenge has been to extend these encouraging results to treatment of more common solid tumors in humans. Strategies that employ high LET radiation emitted by α-particles or Auger electrons may provide a route to increasing the potency of RIT for cancer treatment while minimizing normal tissue toxicity, particularly on hematopoietic stem cells in the BM. However, due to the micrometer range of α-particles and the subcellular nanometer range of Auger electrons, these forms of radiation are most suitable for eradicating individual cancer cells (e.g. leukemia) or micrometastatic or small volume disseminated disease, rather than larger tumor masses. Thus, RIT with high LET radiation would be most valuable to treat minimal residual disease following conventional cancer treatment in order to prevent recurrence or progression, and thereby improve patient outcome. In this clinical scenario, RIT would provide an important advance in cancer treatment. The increasing availability of many humanized or fully human mAbs for treating malignancies has created the opportunity to design second-generation RIT agents complexed to high LET α-particle or Auger electron emitters that could be administered in multiple fractionated doses to improve tumor response. There is a growing sense among investigators in the field that a renaissance may be on the horizon for RIT!

## Acknowledgments

A.J.B. is the recipient of a scholarship from the Terry Fox Foundation-Canadian Institutes of Health Research Excellence in Radiation Research for the 21st Century (EIRR21) Strategic Training Program. S.A. is the recipient of the MDS Nordion Graduate Scholarship in Radiopharmaceutical Sciences. R.M.R. acknowledges research support from the Canadian Institutes of Health Research, Canadian Breast Cancer Foundation (Ontario Region), Canadian Cancer Society Research Institute, Cancer Research Society, the Natural Sciences and Engineering Research Council of Canada and the Ontario Institute for Cancer Research with funds from the Province of Ontario. Figs. 1–3 were designed by Priya Panchal-Banerjee at Priya Visuals (priyavisuals.com).

## References

[1] S.M. Larson, J.A. Carrasquillo, N.K. Cheung, O.W. Press, Radioimmunotherapy of human tumours, Nat. Rev. Cancer 15 (2015) 347–360.
[2] T.E. Witzig, L.I. Gordon, F. Cabanillas, M.S. Czuczman, C. Emmanouilides, R. Joyce, B.L. Pohlman, N.L. Bartlett, G.A. Wiseman, N. Padre, A.J. Grillo-Lopez, P. Multani, C.A. White, Randomized controlled trial of yttrium-90-labeled ibritumomab tiuxetan radioimmunotherapy versus rituximab immunotherapy for patients with relapsed or refractory low-grade, follicular, or transformed B-cell non-Hodgkin's lymphoma, J. Clin. Oncol. 20 (2002) 2453–2463.
[3] M.S. Kaminski, A.D. Zelenetz, O.W. Press, M. Saleh, J. Leonard, L. Fehrenbacher, T.A. Lister, R.J. Stagg, G.F. Tidmarsh, S. Kroll, R.L. Wahl, S.J. Knox, J.M. Vose, Pivotal study of iodine I$^{131}$ tositumomab for chemotherapy-refractory low-grade or transformed low-grade B-cell non-Hodgkin's lymphomas, J. Clin. Oncol. 19 (2001) 3918–3928.
[4] D. Ribatti, From the discovery of monoclonal antibodies to their therapeutic application: an historical reappraisal, Immunol. Lett. 161 (2014) 96–99.
[5] S.M. Larson, Choosing the right radionuclide and antibody for intraperitoneal radioimmunotherapy, J. Natl. Cancer Inst. 83 (1991) 1602–1604.
[6] C. Seidl, Radioimmunotherapy with alpha-particle-emitting radionuclides, Immunotherapy 6 (2014) 431–458.
[7] J. Elgqvist, S. Frost, J.P. Pouget, P. Albertsson, The potential and hurdles of targeted alpha therapy — clinical trials and beyond, Front. Oncol. 3 (2014) 324.
[8] K.E. Baidoo, K. Yong, M.W. Brechbiel, Molecular pathways: targeted alpha-particle radiation therapy, Clin. Cancer Res. 19 (2013) 530–537.
[9] H. Song, R.F. Hobbs, R. Vajravelu, D.L. Huso, C. Esaias, C. Apostolidis, A. Morgenstern, G. Sgouros, Radioimmunotherapy of breast cancer metastases with alpha-particle emitter $^{225}$Ac: comparing efficacy with $^{213}$Bi and $^{90}$Y, Cancer Res. 69 (2009) 8941–8948.
[10] N. Abbas, H. Heyerdahl, O.S. Bruland, E.M. Brevik, J. Dahle, Comparing high LET $^{227}$Th- and low LET $^{177}$Lu-trastuzumab in mice with HER-2 positive SKBR-3 xenografts, Curr. Radiopharm. 6 (2013) 78–86.
[11] M.R. McDevitt, D. Ma, L.T. Lai, J. Simon, P. Borchardt, R.K. Frank, K. Wu, V. Pellegrini, M.J. Curcio, M. Miederer, N.H. Bander, D.A. Scheinberg, Tumor therapy with targeted atomic nanogenerators, Science 294 (2001) 1537–1540.
[12] M. Miederer, M.R. McDevitt, G. Sgouros, K. Kramer, N.K.V. Cheung, D.A. Scheinberg, Pharmacokinetics, dosimetry, and toxicity of the targetable atomic generator, $^{225}$Ac-HuM195, in nonhuman primates, J. Nucl. Med. 45 (2004) 129–137.
[13] J. Schwartz, J.S. Jaggi, J.A. O'Donoghue, S. Ruan, M. McDevitt, S.M. Larson, D.A. Scheinberg, J.L. Humm, Renal uptake of bismuth-213 and its contribution to kidney radiation dose following administration of actinium-225-labeled antibody, Phys. Med. Biol. 56 (2011) 721–733.
[14] J. Jurcic, F. Ravandi, J. Pagel, J.H. Park, B.D. Smith, D. Douer, M.Y. Levy, E. Estey, H.M. Kantarjian, D. Earle, Phase I trial of α-particle therapy with actinium-225 ($^{225}$Ac)-lintuzumab (anti-CD33) and low-dose cytarabine (LDAC) in older patients with untreated acute myeloid leukemia (AML), J. Clin. Oncol. 33 (Suppl. 1) (2015) 7050 [Abstract].
[15] M.R. McDevitt, G. Sgouros, R.D. Finn, J.L. Humm, J.G. Jurcic, S.M. Larson, D.A. Scheinberg, Radioimmunotherapy with alpha-emitting nuclides, Eur. J. Nucl. Med. 25 (1998) 1341–1351.
[16] C. Soyland, S.P. Hassfjell, Survival of human lung epithelial cells following in vitro alpha-particle irradiation with absolute determination of the number of alpha-particle traversals of individual cells, Int. J. Radiat. Biol. 76 (2000) 1315–1322.
[17] C. Wulbrand, C. Seidl, F.C. Gaertner, F. Bruchertseifer, A. Morgenstern, M. Essler, R. Senekowitsch-Schmidtke, Alpha-particle emitting $^{213}$Bi-anti-EGFR immunoconjugates eradicate tumor cells independent of oxygenation, PLoS One 8 (2013), e64730.
[18] M.R. Horsman, L.S. Mortensen, J.B. Petersen, M. Busk, J. Overgaard, Imaging hypoxia to improve radiotherapy outcome, Nat. Rev. Clin. Oncol. 9 (2012) 674–687.
[19] K.J. Yong, D.E. Milenic, K.E. Baidoo, M.W. Brechbiel, $^{212}$Pb-radioimmunotherapy induces G(2) cell-cycle arrest and delays DNA damage repair in tumor xenografts in a model for disseminated intraperitoneal disease, Mol. Cancer Ther. 11 (2012) 639–648.
[20] E. Dadachova, N. Carrasco, The Na/I symporter (NIS): imaging and therapeutic applications, Semin. Nucl. Med. 34 (2004) 23–31.
[21] H. Andersson, E. Cederkrantz, T. Back, C. Divgi, J. Elgqvist, J. Himmelman, G. Horvath, L. Jacobsson, H. Jensen, S. Lindegren, S. Palm, R. Hultborn, Intraperitoneal alpha-particle radioimmunotherapy of ovarian cancer patients: pharmacokinetics and dosimetry of $^{211}$At-MX35 F(ab′)$_2$ — a phase I study, J. Nucl. Med. 50 (2009) 1153–1160.
[22] F. Guérard, J. Gestin, M.W. Brechbiel, Production of [$^{211}$At]-astatinated radiopharmaceuticals and applications in targeted α-particle therapy, Cancer Biother. Radiopharm. 1 (2013) 1–20.
[23] F. Haddad, J. Barbet, J.F. Chatal, The ARRONAX project, Curr. Radiopharm. 4 (2011) 186–196.
[24] R.M. Reilly, J. Sandhu, T.M. varez-Diez, S. Gallinger, J. Kirsh, H. Stern, Problems of delivery of monoclonal antibodies. Pharmaceutical and pharmacokinetic solutions, Clin. Pharmacokinet. 28 (1995) 126–142.
[25] T.K. Nikula, M.R. McDevitt, R.D. Finn, C. Wu, R.W. Kozak, K. Garmestani, M.W. Brechbiel, M.J. Curcio, C.G. Pippin, L. Tiffany-Jones, M.W. Geerlings Sr., C. Apostolidis, R. Molinet, M.W. Geerlings Jr., O.A. Gansow, D.A. Scheinberg, Alpha-emitting bismuth cyclohexylbenzyl DTPA constructs of recombinant humanized anti-CD33 antibodies: pharmacokinetics, bioactivity, toxicity and chemistry, J. Nucl. Med. 40 (1999) 166–176.
[26] D.E. Milenic, M. Roselli, S. Mirzadeh, C.G. Pippin, O.A. Gansow, D. Colcher, M.W. Brechbiel, J. Schlom, In vivo evaluation of bismuth-labeled monoclonal antibody comparing DTPA-derived bifunctional chelates, Cancer Biother. Radiopharm. 16 (2001) 133–146.
[27] S.M. Abbas Rizvi, E.Y. Song, C. Raja, J. Beretov, A. Morgenstern, C. Apostolidis, P.J. Russell, J.H. Kearsley, K. Abbas, B.J. Allen, Preparation and testing of bevacizumab radioimmunoconjugates with bismuth-213 and bismuth-205/bismuth-206, Cancer Biol. Ther. 7 (2008) 1547–1554.
[28] C.S. Kang, H.A. Song, D.E. Milenic, K.E. Baidoo, M.W. Brechbiel, H.S. Chong, Preclinical evaluation of NETA-based bifunctional ligand for radioimmunotherapy applications using $^{212}$Bi and $^{213}$Bi: radiolabeling, serum stability, and biodistribution and tumor uptake studies, Nucl. Med. Biol. 40 (2013) 600–605.
[29] R.A. Julian, C.S. Kang, X. Sun, H.A. Song, E. Revskaya, H.-S. Chong, Optimizing radioimmunotherapy techniques for the alpha-emitter 225Actinium, Proceedings of the 106th Annual Meeting of the American Association for Cancer Research, 2015 ([Abstract 3349]).
[30] M. Pruszynski, M. Lyczko, A. Bilewicz, M.R. Zalutsky, Stability and in vivo behavior of Rh[16aneS4-diol]$^{211}$At complex: a potential precursor for astatine radiopharmaceuticals, Nucl. Med. Biol. 42 (2015) 439–445.

Please cite this article as: S. Aghevlian, et al., Radioimmunotherapy of cancer with high linear energy transfer (LET) radiation delivered by radionuclides emitting α-particles or ..., Adv. Drug Deliv. Rev. (2015), http://dx.doi.org/10.1016/j.addr.2015.12.003

[31] R.M. de Kruijff, H.T. Wolterbeek, A.G. Denkova, A critical review of alpha radionuclide therapy-how to deal with recoiling daughters? Pharm. (Basel) 8 (2015) 321–336.

[32] J.S. Jaggi, B.J. Kappel, M.R. McDevitt, G. Sgouros, C.D. Flombaum, C. Cabassa, D.A. Scheinberg, Efforts to control the errant products of a targeted in vivo generator, Cancer Res. 65 (2005) 4888–4895.

[33] W.F. Maguire, M.R. McDevitt, P.M. Smith-Jones, D.A. Scheinberg, Efficient 1-step radiolabeling of monoclonal antibodies to high specific activity with $^{225}$Ac for alpha-particle radioimmunotherapy of cancer, J. Nucl. Med. 55 (2014) 1492–1498.

[34] R.F. Meredith, J. Torgue, M.T. Azure, S. Shen, S. Saddekni, E. Banaga, R. Carlise, P. Bunch, D. Yoder, R. Alvarez, Pharmacokinetics and imaging of $^{212}$Pb-TCMC-trastuzumab after intraperitoneal administration in ovarian cancer patients, Cancer Biother. Radiopharm. 29 (2014) 12–17.

[35] R. Meredith, J. Torgue, S. Shen, D.R. Fisher, E. Banaga, P. Bunch, D. Morgan, J. Fan, J.M. Straughn Jr., Dose escalation and dosimetry of first-in-human alpha radioimmunotherapy with $^{212}$Pb-TCMC-trastuzumab, J. Nucl. Med. 55 (2014) 1636–1642.

[36] M.R. Zalutsky, D.A. Reardon, G. Akabani, R.E. Coleman, A.H. Friedman, H.S. Friedman, R.E. McLendon, T.Z. Wong, D.D. Bigner, Clinical experience with alpha-particle emitting $^{211}$At: treatment of recurrent brain tumor patients with $^{211}$At-labeled chimeric antitenascin monoclonal antibody 81C6, J. Nucl. Med. 49 (2008) 30–38.

[37] P.E. Borchardt, R.R. Yuan, M. Miederer, M.R. McDevitt, D.A. Scheinberg, Targeted actinium-225 in vivo generators for therapy of ovarian cancer, Cancer Res. 63 (2003) 5084–5090.

[38] M. Miederer, M.R. McDevitt, P. Borchardt, I. Bergman, K. Kramer, N.K. Cheung, D.A. Scheinberg, Treatment of neuroblastoma meningeal carcinomatosis with intrathecal application of alpha-emitting atomic nanogenerators targeting disialoganglioside GD2, Clin. Cancer Res. 10 (2004) 6985–6992.

[39] F.E. Escorcia, E. Henke, M.R. McDevitt, C.H. Villa, P. Smith-Jones, R.G. Blasberg, R. Benezra, D.A. Scheinberg, Selective killing of tumor neovasculature paradoxically improves chemotherapy delivery to tumors, Cancer Res. 70 (2010) 9277–9286.

[40] M.R. Zalutsky, M. Pruszynski, Astatine-211: production and availability, Curr. Radiopharm. 4 (2011) 177–185.

[41] S. Palm, T. Back, I. Claesson, A. Danielsson, J. Elgqvist, S. Frost, R. Hultborn, H. Jensen, S. Lindegren, L. Jacobsson, Therapeutic efficacy of astatine-211-labeled trastuzumab on radioresistant SKOV-3 tumors in nude mice, Int. J. Radiat. Oncol. Biol. Phys. 69 (2007) 572–579.

[42] J. Elgqvist, H. Andersson, T. Back, I. Claesson, R. Hultborn, H. Jensen, B.R. Johansson, S. Lindegren, M. Olsson, S. Palm, E. Warnhammar, L. Jacobsson, Alpha-radioimmunotherapy of intraperitoneally growing OVCAR-3 tumors of variable dimensions: outcome related to measured tumor size and mean absorbed dose, J. Nucl. Med. 47 (2006) 1342–1350.

[43] J. Elgqvist, H. Andersson, T. Back, I. Claesson, R. Hultborn, H. Jensen, S. Lindegren, M. Olsson, S. Palm, E. Warnhammar, L. Jacobsson, Fractionated radioimmunotherapy of intraperitoneally growing ovarian cancer in nude mice with $^{211}$At-MX35 F(ab′)$_2$: therapeutic efficacy and myelotoxicity, Nucl. Med. Biol. 33 (2006) 1065–1072.

[44] J. Elgqvist, H. Andersson, P. Bernhardt, T. Back, I. Claesson, R. Hultborn, H. Jensen, B.R. Johansson, S. Lindegren, M. Olsson, S. Palm, E. Warnhammar, L. Jacobsson, Administered activity and metastatic cure probability during radioimmunotherapy of ovarian cancer in nude mice with $^{211}$At-MX35 F(ab′)$_2$, Int. J. Radiat. Oncol. Biol. Phys. 66 (2006) 1228–1237.

[45] J. Elgqvist, H. Andersson, T. Back, R. Hultborn, H. Jensen, B. Karlsson, S. Lindegren, S. Palm, E. Warnhammar, L. Jacobsson, Therapeutic efficacy and tumor dose estimations in radioimmunotherapy of intraperitoneally growing OVCAR-3 cells in nude mice with $^{211}$At-labeled monoclonal antibody MX35, J. Nucl. Med. 46 (2005) 1907–1915.

[46] H. Andersson, S. Palm, S. Lindegren, T. Back, L. Jacobsson, G. Leser, G. Horvath, Comparison of the therapeutic efficacy of $^{211}$At- and $^{131}$I-labelled monoclonal antibody MOv18 in nude mice with intraperitoneal growth of human ovarian cancer, Anticancer Res. 21 (2001) 409–412.

[47] H. Andersson, S. Lindegren, T. Back, L. Jacobsson, G. Leser, G. Horvath, The curative and palliative potential of the monoclonal antibody MOv18 labelled with $^{211}$At in nude mice with intraperitoneally growing ovarian cancer xenografts — a long-term study, Acta Oncol. 39 (2000) 741–745.

[48] H. Andersson, S. Lindegren, T. Back, L. Jacobsson, G. Leser, G. Horvath, Radioimmunotherapy of nude mice with intraperitoneally growing ovarian cancer xenograft utilizing $^{211}$At-labelled monoclonal antibody MOv18, Anticancer Res. 20 (2000) 459–462.

[49] M.R. Zalutsky, M.G. Stabin, R.H. Larsen, D.D. Bigner, Tissue distribution and radiation dosimetry of astatine-211-labeled chimeric 81C6, an alpha-particle-emitting immunoconjugate, Nucl. Med. Biol. 24 (1997) 255–261.

[50] S.E. Eriksson, T. Back, E. Elgstrom, H. Jensen, R. Nilsson, S. Lindegren, J. Tennvall, Successful radioimmunotherapy of established syngeneic rat colon carcinoma with $^{211}$At-mAb, EJNMMI Res. 3 (2013) 23.

[51] J.J. Orozco, T. Bäck, A. Kenoyer, E.R. Balkin, D.K. Hamlin, D.S. Wilbur, D.R. Fisher, S.L. Frayo, M.D. Hylarides, D.J. Green, A.K. Gopal, O.W. Press, J.M. Pagel, Anti-CD45 radioimmunotherapy using $^{211}$At with bone marrow transplantation prolongs survival in a disseminated murine leukemia model, Blood 121 (2013) 3759–3767.

[52] R.W. Kozak, R.W. Atcher, O.A. Gansow, A.M. Friedman, J.J. Hines, T.A. Waldmann, Bismuth-212-labeled anti-Tac monoclonal antibody: alpha-particle-emitting radionuclides as modalities for radioimmunotherapy, Proc. Natl. Acad. Sci. U. S. A. 83 (1986) 474–478.

[53] F. Hartmann, E.M. Horak, K. Garmestani, C. Wu, M.W. Brechbiel, R.W. Kozak, J. Tso, S.A. Kosteiny, O.A. Gansow, D.L. Nelson, T.A. Waldmann, Radioimmunotherapy of nude mice bearing a human interleukin 2 receptor alpha-expressing lymphoma utilizing the alpha-emitting radionuclide-conjugated monoclonal antibody $^{212}$Bi-anti-Tac, Cancer Res. 54 (1994) 4362–4370.

[54] R.B. Huneke, C.G. Pippin, R.A. Squire, M.W. Brechbiel, O.A. Gansow, M. Strand, Effective alpha-particle-mediated radioimmunotherapy of murine leukemia, Cancer Res. 52 (1992) 5818–5820.

[55] D.E. Milenic, K. Garmestani, E.D. Brady, P.S. Albert, D. Ma, A. Abdulla, M.W. Brechbiel, Alpha-particle radioimmunotherapy of disseminated peritoneal disease using a $^{212}$Pb-labeled radioimmunoconjugate targeting HER2, Cancer Biother. Radiopharm. 20 (2005) 557–568.

[56] D.E. Milenic, K. Garmestani, E.D. Brady, P.S. Albert, A. Abdulla, J. Flynn, M.W. Brechbiel, Potentiation of high-LET radiation by gemcitabine: targeting HER2 with trastuzumab to treat disseminated peritoneal disease, Clin. Cancer Res. 13 (2007) 1926–1935.

[57] D.E. Milenic, K.E. Baidoo, Y.S. Kim, M.W. Brechbiel, Evaluation of cetuximab as a candidate for targeted alpha-particle radiation therapy of HER1-positive disseminated intraperitoneal disease, MAbs 7 (2015) 255–264.

[58] P.A. Burke, S.J. DeNardo, L.A. Miers, D.L. Kukis, G.L. DeNardo, Combined modality radioimmunotherapy. Promise and peril, Cancer 94 (2002) 1320–1331.

[59] D.E. Milenic, K. Garmestani, E.D. Brady, K.E. Baidoo, P.S. Albert, K.J. Wong, J. Flynn, M.W. Brechbiel, Multimodality therapy: potentiation of high linear energy transfer radiation with paclitaxel for the treatment of disseminated peritoneal disease, Clin. Cancer Res. 14 (2008) 5108–5115.

[60] D.E. Milenic, K.E. Baidoo, J.H. Shih, K.J. Wong, M.W. Brechbiel, Evaluation of platinum chemotherapy in combination with HER2-targeted alpha-particle radiation, Cancer Biother. Radiopharm. 28 (2013) 441–449.

[61] Z. Tan, P. Chen, N. Schneider, S. Glover, L. Cui, J. Torgue, O. Rixe, H.B. Spitz, Z. Dong, Significant systemic therapeutic effects of high-LET immunoradiation by $^{212}$Pb-trastuzumab against prostatic tumors of androgen-independent human prostate cancer in mice, Int. J. Oncol. 40 (2012) 1881–1888.

[62] D.E. Milenic, A.A. Molinolo, M.S. Solivella, E. Banaga, J. Torgue, S. Besnainou, M.W. Brechbiel, K.E. Baidoo, Toxicological studies of $^{212}$Pb intravenously or intraperitoneally injected into mice for a phase 1 trial, Pharm. (Basel) 8 (2015) 416–434.

[63] M. Cherel, S. Gouard, J. Gaschet, C. Sai-Maurel, F. Bruchertseifer, A. Morgenstern, M. Bourgeois, J.F. Gestin, F.K. Bodere, J. Barbet, P. Moreau, F. Davodeau, 213Bi radioimmunotherapy with an anti-mCD138 monoclonal antibody in a murine model of multiple myeloma, J. Nucl. Med. 54 (2013) 1597–1604.

[64] H. Song, M. Hedayati, R.F. Hobbs, C. Shao, F. Bruchertseifer, A. Morgenstern, T.L. Deweese, G. Sgouros, Targeting aberrant DNA double-strand break repair in triple-negative breast cancer with alpha-particle emitter radiolabeled anti-EGFR antibody, Mol. Cancer Ther. 12 (2013) 2043–2054.

[65] D. Milenic, K. Garmestani, E. Dadachova, L. Chappell, P. Albert, D. Hill, J. Schlom, M. Brechbiel, Radioimmunotherapy of human colon carcinoma xenografts using a 213Bi-labeled domain-deleted humanized monoclonal antibody, Cancer Biother. Radiopharm. 19 (2004) 135–147.

[66] C. Friesen, G. Glatting, B. Koop, K. Schwarz, A. Morgenstern, C. Apostolidis, K.M. Debatin, S.N. Reske, Breaking chemoresistance and radioresistance with [213Bi]anti-CD45 antibodies in leukemia cells, Cancer Res. 67 (2007) 1950–1958.

[67] R. Beck, C. Seidl, B. Pfost, A. Morgenstern, F. Bruchertseifer, H. Baum, M. Schwaiger, R. Senekowitsch-Schmidtke, $^{213}$Bi-radioimmunotherapy defeats early-stage disseminated gastric cancer in nude mice, Cancer Sci. 98 (2007) 1215–1222.

[68] B. Pfost, C. Seidl, M. Autenrieth, D. Saur, F. Bruchertseifer, A. Morgenstern, M. Schwaiger, R. Senekowitsch-Schmidtke, Intravesical alpha-radioimmunotherapy with 213Bi-anti-EGFR-mAb defeats human bladder carcinoma in xenografted nude mice, J. Nucl. Med. 50 (2009) 1700–1708.

[69] J. Fazel, S. Rotzer, C. Seidl, B. Feuerecker, M. Autenrieth, G. Weirich, F. Bruchertseifer, A. Morgenstern, R. Senekowitsch-Schmidtke, Fractionated intravesical radioimmunotherapy with Bi-anti-EGFR-MAb is effective without toxic side-effects in a nude mouse model of advanced human bladder carcinoma, Cancer Biol. Ther. 1–9 (2015).

[70] B.J. Allen, S.M. Rizvi, C.F. Qu, R.C. Smith, Targeted alpha therapy approach to the management of pancreatic cancer, Cancers (Basel) 3 (2011) 1821–1843.

[71] J.G. Jurcic, S.M. Larson, G. Sgouros, M.R. McDevitt, R.D. Finn, C.R. Divgi, A.M. Ballangrud, K.A. Hamacher, D. Ma, J.L. Humm, M.W. Brechbiel, R. Molinet, D.A. Scheinberg, Targeted alpha particle immunotherapy for myeloid leukemia, Blood 100 (2002) 1233–1239.

[72] T.L. Rosenblat, M.R. McDevitt, D.A. Mulford, N. Pandit-Taskar, C.R. Divgi, K.S. Panageas, M.L. Heaney, S. Chanel, A. Morgenstern, G. Sgouros, S.M. Larson, D.A. Scheinberg, J.G. Jurcic, Sequential cytarabine and alpha-particle immunotherapy with bismuth-213-lintuzumab (HuM195) for acute myeloid leukemia, Clin. Cancer Res. 16 (2010) 5303–5311.

[73] D.E. Milenic, E.D. Brady, K. Garmestani, P.S. Albert, A. Abdulla, M.W. Brechbiel, Improved efficacy of alpha-particle-targeted radiation therapy: dual targeting of human epidermal growth factor receptor-2 and tumor-associated glycoprotein 72, Cancer 116 (2010) 1059–1066.

[74] N. Abbas, H. Heyerdahl, O.S. Bruland, J. Borrebaek, J. Nesland, J. Dahle, Experimental alpha-particle radioimmunotherapy of breast cancer using $^{227}$Th-labeled p-benzyl-DOTA-trastuzumab, EJNMMI Res. 1 (2011) 18.

[75] P. Auger, Sur les rayons β secondaires produit dans un gaz par des rayons X, Comp. Rend. 180 (1925) 65–68.

[76] R.M. Reilly, A. Kassis, Targeted Auger electron radiotherapy of malignancies, in: R.M. Reilly (Ed.), Monoclonal Antibody and Peptide-Targeted Radiotherapy of Cancer, John Wiley & Sons Inc., Hoboken 2010, pp. 289–348.

[77] A.I. Kassis, Therapeutic radionuclides: biophysical and radiobiologic principles, Semin. Nucl. Med. 38 (2008) 358–366.

[78] A.I. Kassis, K.S. Sastry, S.J. Adelstein, Kinetics of uptake, retention, and radiotoxicity of $^{125}$IUdR in mammalian cells: implications of localized energy deposition by Auger processes, Radiat. Res. 109 (1987) 78–89.


Please cite this article as: S. Aghevlian, et al., Radioimmunotherapy of cancer with high linear energy transfer (LET) radiation delivered by radionuclides emitting α-particles or ..., Adv. Drug Deliv. Rev. (2015), http://dx.doi.org/10.1016/j.addr.2015.12.003

[79] G.M. Makrigiorgos, A.I. Kassis, J. Baranowska-Kortylewicz, K.D. McElvany, M.J. Welch, K.S. Sastry, S.J. Adelstein, Radiotoxicity of 5-[$^{123}$I]iodo-2′-deoxyuridine in V79 cells: a comparison with 5-[$^{125}$I]iodo-2′-deoxyuridine, Radiat. Res. 118 (1989) 532–544.
[80] A.I. Kassis, F. Fayad, B.M. Kinsey, K.S. Sastry, R.A. Taube, S.J. Adelstein, Radiotoxicity of $^{125}$I in mammalian cells, Radiat. Res. 111 (1987) 305–318.
[81] A.I. Kassis, S.J. Adelstein, C. Haydock, K.S. Sastry, Thallium-201: an experimental and a theoretical radiobiological approach to dosimetry, J. Nucl. Med. 24 (1983) 1164–1175.
[82] K.G. Hofer, C.R. Harris, J.M. Smith, Rdiotoxicity of intracellular $^{67}$Ga, $^{125}$I and $^{3}$H. Nuclear versus cytoplasmic radiation effects in murine L1210 leukaemia, Int. J. Radiat. Biol. Relat. Stud. Phys. Chem. Med. 28 (1975) 225–241.
[83] N. Miyazaki, K. Shinohara, Cell killing induced by decay of $^{125}$I during the cell cycle: comparison of $^{125}$I-antipyrine with $^{125}$I-bovine serum albumin, Radiat. Res. 133 (1993) 182–186.
[84] R.L. Warters, K.G. Hofer, C.R. Harris, J.M. Smith, Radionuclide toxicity in cultured mammalian cells: elucidation of the primary site of radiation damage, Curr. Top. Radiat. Res. Q. 12 (1978) 389–407.
[85] E. Pomplun, J. Booz, D.E. Charlton, A Monte Carlo simulation of Auger cascades, Radiat. Res. 111 (1987) 533–552.
[86] A.I. Kassis, R.S. Harapanhalli, S.J. Adelstein, Comparison of strand breaks in plasmid DNA after positional changes of Auger electron-emitting iodine-125, Radiat. Res. 151 (1999) 167–176.
[87] A.I. Kassis, R.S. Harapanhalli, S.J. Adelstein, Strand breaks in plasmid DNA after positional changes of Auger electron-emitting iodine-125: direct compared to indirect effects, Radiat. Res. 152 (1999) 530–538.
[88] A. Fasih, H. Fonge, Z. Cai, J.V. Leyton, I. Tikhomirov, S.J. Done, R.M. Reilly, $^{111}$In-Bn-DTPA-nimotuzumab with/without modification with nuclear translocation sequence (NLS) peptides: an Auger electron-emitting radioimmunotherapeutic agent for EGFR-positive and trastuzumab (Herceptin)-resistant breast cancer, Breast Cancer Res. Treat. 135 (2012) 189–200.
[89] P. Chen, J. Wang, K. Hope, L. Lin, J. Dick, R. Cameron, J. Brandwein, M. Minden, R.M. Reilly, Nuclear localizing sequences (NLS) promote nuclear translocation and enhance the radiotoxicity of the anti-CD33 monoclonal antibody HuM195 labeled with $^{111}$In in human myeloid leukemia cells, J. Nucl. Med. 47 (2006) 827–836.
[90] D.L. Costantini, C. Chan, Z. Cai, K.A. Vallis, R.M. Reilly, $^{111}$In-labeled trastuzumab (Herceptin) modified with nuclear localization sequences (NLS): an Auger electron-emitting radiotherapeutic agent for HER2/neu-amplified breast cancer, J. Nucl. Med. 48 (2007) 1357–1368.
[91] D.L. Costantini, M. Hu, R.M. Reilly, Peptide motifs for insertion of radiolabeled biomolecules into cells and routing to the nucleus for cancer imaging or radiotherapeutic applications, Cancer Biother. Radiopharm. 23 (2008) 3–24.
[92] J.P. Pouget, L. Santoro, L. Raymond, N. Chouin, M. Bardies, C. Bascoul-Mollevi, H. Huguet, D. Azria, P.O. Kotzki, M. Pelegrin, E. Vives, A. Pelegrin, Cell membrane is a more sensitive target than cytoplasm to dense ionization produced by auger electrons, Radiat. Res. 170 (2008) 192–200.
[93] J.P. Pouget, C. Lozza, E. Deshayes, V. Boudousq, I. Navarro-Teulon, Introduction to radiobiology of targeted radionuclide therapy, Front. Med. 2 (2015) 12.
[94] I. Corre, C. Niaudet, F. Paris, Plasma membrane signaling induced by ionizing radiation, Mutat. Res. 704 (2010) 61–67.
[95] R.N. Kolesnick, A. Haimovitz-Friedman, Z. Fuks, The sphingomyelin signal transduction pathway mediates apoptosis for tumor necrosis factor, Fas, and ionizing radiation, Biochem. Cell Biol. 72 (1994) 471–474.
[96] A. Haimovitz-Friedman, Radiation-induced signal transduction and stress response, Radiat. Res. 150 (1998) 102–108.
[97] R.M. Reilly, Biomolecules as targeting vehicles for in situ radiotherapy of malignancies, in: J. Knaeblein, R. Mueller (Eds.), Modern Biopharmaceuticals: Design, Development and Optimization, Weinheim, Wiley-VCH. 2005, pp. 497–526.
[98] M. Boyd, A. Sorensen, A.G. McCluskey, R.J. Mairs, Radiation quality-dependent bystander effects elicited by targeted radionuclides, J. Pharm. Pharmacol. 60 (2008) 951–958.
[99] L.Y. Xue, N.J. Butler, G.M. Makrigiorgos, S.J. Adelstein, A.I. Kassis, Bystander effect produced by radiolabeled tumor cells in vivo, Proc. Natl. Acad. Sci. U. S. A. 99 (2002) 13765–13770.
[100] H. Kishikawa, K. Wang, S.J. Adelstein, A.I. Kassis, Inhibitory and stimulatory bystander effects are differentially induced by Iodine-125 and Iodine-123, Radiat. Res. 165 (2006) 688–694.
[101] M. Boyd, S.C. Ross, J. Dorrens, N.E. Fullerton, K.W. Tan, M.R. Zalutsky, R.J. Mairs, Radiation-induced biologic bystander effect elicited in vitro by targeted radiopharmaceuticals labeled with alpha-, beta-, and auger electron-emitting radionuclides, J. Nucl. Med. 47 (2006) 1007–1015.
[102] Z. Cai, J.P. Pignol, C. Chan, R.M. Reilly, Cellular dosimetry of $^{111}$In using monte carlo N-particle computer code: comparison with analytic methods and correlation with in vitro cytotoxicity, J. Nucl. Med. 51 (2010) 462–470.
[103] R.B. Michel, M.E. Castillo, P.M. Andrews, M.J. Mattes, In vitro toxicity of A-431 carcinoma cells with antibodies to epidermal growth factor receptor and epithelial glycoprotein-1 conjugated to radionuclides emitting low-energy electrons, Clin. Cancer Res. 10 (2004) 5957–5966.
[104] D.L. Costantini, K. McLarty, H. Lee, S.J. Done, K.A. Vallis, R.M. Reilly, Antitumor effects and normal-tissue toxicity of $^{111}$In-nuclear localization sequence-trastuzumab in athymic mice bearing HER-positive human breast cancer xenografts, J. Nucl. Med. 51 (2010) 1084–1091.
[105] M.E. Caplin, W. Mielcarek, J.R. Buscombe, A.L. Jones, P.L. Croasdale, M.S. Cooper, A.K. Burroughs, A.W. Hilson, Toxicity of high-activity $^{111}$In-octreotide therapy in patients with disseminated neuroendocrine tumours, Nucl. Med. Commun. 21 (2000) 97–102.
[106] M. Ychou, D. Azria, C. Menkarios, P. Faurous, F. Quenet, B. Saint-Aubert, P. Rouanet, M. Pelegrin, C. Bascoul-Mollevi, D. Guerreau, J.C. Saccavini, J.P. Mach, J.C. Artus, A. Pelegrin, Adjuvant radioimmunotherapy trial with iodine-131-labeled anti-carcinoembryonic antigen monoclonal antibody F6 F(ab′)$_2$ after resection of liver metastases from colorectal cancer, Clin. Cancer Res. 14 (2008) 3487–3493.
[107] M. Ychou, A. Pelegrin, P. Faurous, B. Robert, J.C. Saccavini, D. Guerreau, J.F. Rossi, M. Fabbro, F. Buchegger, J.P. Mach, J.C. Artus, Phase-I/II radio-immunotherapy study with Iodine-131-labeled anti-CEA monoclonal antibody F6 F(ab′)$_2$ in patients with non-resectable liver metastases from colorectal cancer, Int. J. Cancer 75 (1998) 615–619.
[108] F. Buchegger, C. Pfister, K. Fournier, F. Prevel, M. Schreyer, S. Carrel, J.P. Mach, Ablation of human colon carcinoma in nude mice by $^{131}$I-labeled monoclonal anti-carcinoembryonic antigen antibody F(ab′)2 fragments, J. Clin. Invest. 83 (1989) 1449–1456.
[109] S.I. Park, J. Shenoi, J.M. Pagel, D.K. Hamlin, D.S. Wilbur, N. Orgun, A.L. Kenoyer, S. Frayo, A. Axtman, T. Back, Y. Lin, D.R. Fisher, A.K. Gopal, D.J. Green, O.W. Press, Conventional and pretargeted radioimmunotherapy using bismuth-213 to target and treat non-Hodgkin lymphomas expressing CD20: a preclinical model toward optimal consolidation therapy to eradicate minimal residual disease, Blood 116 (2010) 4231–4239.
[110] R.M. Sharkey, H. Karacay, S. Litwin, E.A. Rossi, W.J. McBride, C.H. Chang, D.M. Goldenberg, Improved therapeutic results by pretargeted radioimmunotherapy of non-Hodgkin′s lymphoma with a new recombinant, trivalent, anti-CD20, bispecific antibody, Cancer Res. 68 (2008) 5282–5290.
[111] M.R. Zalutsky, A.S. Narula, A method for the radiohalogenation of proteins resulting in decreased thyroid uptake of radioiodine, Appl. Radiat. Isot. 38 (1987) 1051–1055.
[112] R.M. Reilly, The radiochemistry of monoclonal antibodies and peptides, in: R.M. Reilly (Ed.), Monoclonal Antibody and Peptide-Targeted Radiotherapy of Cancer, John Wiley & Sons, Hoboken 2010, pp. 39–100.
[113] S.A. Prigent, N.R. Lemoine, The type 1 (EGFR-related) family of growth factor receptors and their ligands, Prog. Growth Factor Res. 4 (1992) 1–24.
[114] H.S. Earp, T.L. Dawson, X. Li, H. Yu, Heterodimerization and functional interaction between EGF receptor family members: a new signaling paradigm with implications for breast cancer research, Breast Cancer Res. Treat. 35 (1995) 115–132.
[115] D.S. Salomon, R. Brandt, F. Ciardiello, N. Normanno, Epidermal growth factor-related peptides and their receptors in human malignancies, Crit. Rev. Oncol. Hematol. 19 (1995) 183–232.
[116] R.M. Reilly, P. Chen, J. Wang, D. Scollard, R. Cameron, K.A. Vallis, Preclinical pharmacokinetic, biodistribution, toxicology, and dosimetry studies of 111In-DTPA-human epidermal growth factor: an auger electron-emitting radiotherapeutic agent for epidermal growth factor receptor-positive breast cancer, J. Nucl. Med. 47 (2006) 1023–1031.
[117] R. Dienstmann, B. Markman, J. Tabernero, Application of monoclonal antibodies as cancer therapy in solid tumors, Curr. Clin. Pharmacol. 7 (2012) 137–145.
[118] S.Y. Lin, K. Makino, W. Xia, A. Matin, Y. Wen, K.Y. Kwong, L. Bourguignon, M.C. Hung, Nuclear localization of EGF receptor and its potential new role as a transcription factor, Nat. Cell Biol. 3 (2001) 802–808.
[119] A.M. Traynor, T.L. Weigel, K.R. Oettel, D.T. Yang, C. Zhang, K. Kim, R. Salgia, M. Iida, T.M. Brand, T. Hoang, T.C. Campbell, H.R. Hernan, D.L. Wheeler, Nuclear EGFR protein expression predicts poor survival in early stage non-small cell lung cancer, Lung Cancer 81 (2013) 138–141.
[120] I. Hadzisejdic, E. Mustac, N. Jonjic, M. Petkovic, B. Grahovac, Nuclear EGFR in ductal invasive breast cancer: correlation with cyclin-D1 and prognosis, Mod. Pathol. 23 (2010) 392–403.
[121] Z. Cai, K.A. Vallis, R.M. Reilly, Computational analysis of the number, area and density of gamma-H2AX foci in breast cancer cells to $^{111}$In-DTPA-hEGF or gamma-rays using Image-J software, Int. J. Radiat. Biol. 85 (2009) 262–271.
[122] P. Stanton, S. Richards, J. Reeves, M. Nikolic, K. Edington, L. Clark, G. Robertson, D. Souter, R. Mitchell, F.J. Hendler, et al., Epidermal growth factor receptor expression by human squamous cell carcinomas of the head and neck, cell lines and xenografts, Br. J. Cancer 70 (1994) 427–433.
[123] M.J. Mattes, D.M. Goldenberg, Therapy of human carcinoma xenografts with antibodies to EGFr and HER-2 conjugated to radionuclides emitting low-energy electrons, Eur. J. Nucl. Med. Mol. Imaging 35 (2008) 1249–1258.
[124] H. Bender, H. Takahashi, K. Adachi, P. Belser, S. Liang, M. Prewett, M. Schrappe, A. Sutter, U. Rodeck, D. Herlyne, Immunotherapy of human glioma xenografts with unlabeled, $^{131}$I- or $^{125}$I-labeled monoclonal antibody 425 to epidermal growth factor receptor, Cancer Res. 52 (1992) 121–126.
[125] T.S. Quang, L. Brady, Radioimmunotherapy as a novel treatment regimen: 125 I-labeled monoclonal antibody 425 in the treatment of high-grade brain gliomas, Int. J. Radiat. Oncol. Biol. Phys. 58 (2004) 972–975.
[126] R.M. Reilly, R. Kiarash, R.G. Cameron, N. Porlier, J. Sandhu, R.P. Hill, K. Vallis, A. Hendler, J. Gariepy, $^{111}$In-labeled EGF is selectively radiotoxic to human breast cancer cells overexpressing EGFR, J. Nucl. Med. 41 (2000) 429–438.
[127] Z. Cai, Z. Chen, K.E. Bailey, D.A. Scollard, R.M. Reilly, K.A. Vallis, Relationship between induction of phosphorylated H2AX and survival in breast cancer cells exposed to $^{111}$In-DTPA-hEGF, J. Nucl. Med. 49 (2008) 1353–1361.
[128] M. Hu, D. Scollard, C. Chan, P. Chen, K. Vallis, R.M. Reilly, Effect of the EGFR density of breast cancer cells on nuclear importation, in vitro cytotoxicity, and tumor and normal-tissue uptake of [$^{111}$In]DTPA-hEGF, Nucl. Med. Biol. 34 (2007) 887–896.
[129] P. Chen, R. Cameron, J. Wang, K.A. Vallis, R.M. Reilly, Antitumor effects and normal tissue toxicity of $^{111}$In-labeled epidermal growth factor administered to athymic mice bearing epidermal growth factor receptor-positive human breast cancer xenografts, J. Nucl. Med. 44 (2003) 1469–1478.

Please cite this article as: S. Aghevlian, et al., Radioimmunotherapy of cancer with high linear energy transfer (LET) radiation delivered by radionuclides emitting α-particles or ..., Adv. Drug Deliv. Rev. (2015), http://dx.doi.org/10.1016/j.addr.2015.12.003

[130] T.M. Walz, C. Malm, B.K. Nishikawa, A. Wasteson, Transforming growth factor-alpha (TGF-alpha) in human bone marrow: demonstration of TGF-alpha in erythroblasts and eosinophilic precursor cells and of epidermal growth factor receptors in blastlike cells of myelomonocytic origin, Blood 85 (1995) 2385–2392.
[131] K.A. Vallis, R.M. Reilly, D. Scollard, P. Merante, A. Brade, S. Velauthapillai, C. Caldwell, I. Chan, M. Freeman, G. Lockwood, N.A. Miller, B. Cornelissen, J. Petronis, K. Sabate, Phase I trial to evaluate the tumor and normal tissue uptake, radiation dosimetry and safety of $^{111}$In-DTPA-human epidermal growth factor in patients with metastatic EGFR-positive breast cancer, Am. J. Nucl. Med. Mol. Imaging 4 (2014) 181–192.
[132] O. Abdel-Rahman, M. Fouad, Correlation of cetuximab-induced skin rash and outcomes of solid tumor patients treated with cetuximab: a systematic review and meta-analysis, Crit. Rev. Oncol. Hematol. 93 (2015) 127–135.
[133] C. Panosa, F. Tebar, M. Ferrer-Batalle, H. Fonge, M. Seno, R.M. Reilly, A. Massaguer, R. De Llorens, Development of an epidermal growth factor derivative with EGFR blocking activity, PLoS ONE 8 (2013), e69325.
[134] C. Panosa, H. Fonge, M. Ferrer-Batalle, J.A. Menendez, A. Massaguer, R. De Llorens, R.M. Reilly, A comparison of non-biologically active truncated EGF (EGFt) and full-length hEGF for delivery of Auger electron-emitting $^{111}$In to EGFR-positive breast cancer cells and tumor xenografts in athymic mice, Nucl. Med. Biol. (2015)http://dx.doi.org/10.1016/j.nucmedbio.2015.08.003 (Epub ahead of print).
[135] C.L. Arteaga, M.X. Sliwkowski, C.K. Osborne, E.A. Perez, F. Puglisi, L. Gianni, Treatment of HER2-positive breast cancer: current status and future perspectives, Nat. Rev. Clin. Oncol. 9 (2011) 16–32.
[136] V. Bertelsen, E. Stang, The mysterious ways of ErbB2/HER2 trafficking, Membranes 4 (2014) 424–446.
[137] Y. Xie, M.C. Hung, Nuclear localization of p185 NEU tyrosine kinase and its association with transcriptional activation, Biochem. Biophys. Res. Commun. 203 (1994) 1589–1598.
[138] M. Cuello, A.A. Ettenberg, A.S. Clark, M.M. Keane, R.H. Posner, M.M. Nau, P.A. Dennis, S. Lipkowitz, Down-regulation of the erbB-2 receptor by trastuzumab (Herceptin) enhances tumor necrosis factor-related apoptosis-inducing ligand-mediated apoptosis in breast and ovarian cancer cell lines that overexpress erbB-2, Cancer Res. 61 (2001) 4892–4900.
[139] J. Baselga, J. Albanell, Mechanism of action of anti-HER2 monoclonal antibodies, Ann. Oncol. 12 (2001) 35–41.
[140] J. Baselga, Clinical trials of Herceptin (trastuzumab), Eur. J. Cancer 37 (2001) 18–24.
[141] M. Piccart, Circumventing de novo and acquired resistance to trastuzumab: new hope for the care of ErbB2-positive breast cancer, Clin. Breast Cancer 8 (2008) 100–113.
[142] D.L. Costantini, K. Bateman, K. McLarty, K.A. Vallis, R.M. Reilly, Trastuzumab-resistant breast cancer cells remain sensitive to the auger electron-emitting radiotherapeutic agent $^{111}$In-NLS-trastuzumab and are radiosensitized by methotrexate, J. Nucl. Med. 49 (2008) 1498–1505.
[143] J.M. du Manoir, G. Francia, S. Man, M. Mossoba, J.A. Medin, A. Viloria-Petit, D.J. Hicklin, U. Emmenegger, R.S. Kerbel, Strategies for delaying or treating in vivo acquired resistance to trastuzumab in human breast cancer xenografts, Clin. Cancer Res. 12 (2006) 904–916.
[144] D.L. Costantini, D.F. Villani, K.A. Vallis, R.M. Reilly, Methotrexate, paclitaxel, and doxorubicin radiosensitize HER2-amplified human breast cancer cells to the Auger electron-emitting radiotherapeutic agent $^{111}$In-NLS-trastuzumab, J. Nucl. Med. 51 (2010) 477–483.
[145] Y. Lu, G. Ngo Ndjock Mbong, P. Liu, C. Chan, Z. Cai, D. Weinrich, A.J. Boyle, R.M. Reilly, M.A. Winnik, Synthesis of polyglutamide-based metal-chelating polymers and their site-specific conjugation to trastuzumab for auger electron radioimmunotherapy, Biomacromolecules 15 (2014) 2027–2037.
[146] G. Ngo Ndjock Mbong, Y. Lu, C. Chan, Z. Cai, P. Liu, A.J. Boyle, M.A. Winnik, R.M. Reilly, Trastuzumab labeled to high specific activity with $^{111}$In by site-specific conjugation to a metal-chelating polymer exhibits amplified Auger electron-mediated cytotoxicity on HER2-positive breast cancer cells, Mol. Pharm. 12 (2015) 1951–1960.
[147] C. Chan, Z. Cai, R.M. Reilly, Trastuzumab labeled to high specific activity with $^{111}$In by conjugation to G4 PAMAM dendrimers derivatized with multiple DTPA chelators exhibits increased cytotoxic potency on HER2-positive breast cancer cells, Pharm. Res. 30 (2013) 1999–2009.
[148] B. Hoang, R.M. Reilly, C. Allen, Block copolymer micelles target Auger electron radiotherapy to the nucleus of HER2-positive breast cancer cells, Biomacromolecules 13 (2012) 455–465.
[149] R.B. Michel, P.M. Andrews, M.E. Castillo, M.J. Mattes, In vitro cytotoxicity of carcinoma cells with $^{111}$In-labeled antibodies to HER-2, Mol. Cancer Ther. 4 (2005) 927–937.
[150] J.K. Heath, S.J. White, C.N. Johnstone, B. Catimel, R.J. Simpson, R.L. Moritz, G.F. Tu, H. Ji, R.H. Whitehead, L.C. Groenen, A.M. Scott, G. Ritter, L. Cohen, S. Welt, L.J. Old, E.C. Nice, A.W. Burgess, The human A33 antigen is a transmembrane glycoprotein and a novel member of the immunoglobulin superfamily, Proc. Natl. Acad. Sci. U. S. A. 94 (1997) 469–474.
[151] E.C. Barendswaard, J.L. Humm, J.A. O'Donoghue, G. Sgouros, R.D. Finn, A.M. Scott, S.M. Larson, S. Welt, Relative therapeutic efficacy of $^{125}$I- and $^{131}$I-labeled monoclonal antibody A33 in a human colon cancer xenograft, J. Nucl. Med. 42 (2001) 1251–1256.
[152] T.M. Behr, M. Behe, M. Lohr, G. Sgouros, C. Angerstein, E. Wehrmann, K. Nebendahl, W. Becker, Therapeutic advantages of Auger electron- over beta-emitting radiometals or radioiodine when conjugated to internalizing antibodies, Eur. J. Nucl. Med. 27 (2000) 753–765.
[153] T.M. Behr, G. Sgouros, V. Vougioukas, S. Memtsoudis, S. Gratz, H. Schmidberger, R.D. Blumenthal, D.M. Goldenberg, W. Becker, Therapeutic efficacy and dose-limiting toxicity of Auger-electron vs. beta emitters in radioimmunotherapy with internalizing antibodies: evaluation of $^{125}$I- vs. $^{131}$I-labeled CO17-1A in a human colorectal cancer model, Int. J. Cancer 76 (1998) 738–748.
[154] S. Welt, A.M. Scott, C.R. Divgi, N.E. Kemeny, R.D. Finn, F. Daghighian, J.S. Germain, E.C. Richards, S.M. Larson, L.J. Old, Phase I/II study of iodine 125-labeled monoclonal antibody A33 in patients with advanced colon cancer, J. Clin. Oncol. 14 (1996) 1787–1797.
[155] S. Welt, C.R. Divgi, N. Kemeny, R.D. Finn, A.M. Scott, M. Graham, J.S. Germain, E.C. Richards, S.M. Larson, H.F. Oettgen, et al., Phase I/II study of iodine 131-labeled monoclonal antibody A33 in patients with advanced colon cancer, J. Clin. Oncol. 12 (1994) 1561–1571.
[156] R. Stein, M.J. Mattes, T.M. Cardillo, H.J. Hansen, C.H. Chang, J. Burton, S. Govindan, D.M. Goldenberg, CD74: a new candidate target for the immunotherapy of B-cell neoplasms, Clin. Cancer Res. 13 (2007) 5556–5563.
[157] H.J. Hansen, G.L. Ong, H. Diril, A. Valdez, P.A. Roche, G.L. Griffiths, D.M. Goldenberg, M.J. Mattes, Internalization and catabolism of radiolabelled antibodies to the MHC class-II invariant chain by B-cell lymphomas, Biochem. J. 320 (1996) 293–300.
[158] G.L. Griffiths, S.V. Govindan, G. Sgouros, G.L. Ong, D.M. Goldenberg, M.J. Mattes, Cytotoxicity with Auger electron-emitting radionuclides delivered by antibodies, Int. J. Cancer 81 (1999) 985–992.
[159] S.V. Govindan, D.M. Goldenberg, S.E. Elsamra, G.L. Griffiths, G.L. Ong, M.W. Brechbiel, J. Burton, G. Sgouros, M.J. Mattes, Radionuclides linked to a CD74 antibody as therapeutic agents for B-cell lymphoma: comparison of Auger electron emitters with beta-particle emitters, J. Nucl. Med. 41 (2000) 2089–2097.
[160] G.L. Ong, S.E. Elsamra, D.M. Goldenberg, M.J. Mattes, Single-cell cytotoxicity with radiolabeled antibodies, Clin. Cancer Res. 7 (2001) 192–201.
[161] R. Ochakovskaya, L. Osorio, D.M. Goldenberg, M.J. Mattes, Therapy of disseminated B-cell lymphoma xenografts in severe combined immunodeficient mice with an anti-CD74 antibody conjugated with $^{111}$indium, $^{67}$gallium, or $^{90}$yttrium, Clin. Cancer Res. 7 (2001) 1505–1510.
[162] R.B. Michel, M.W. Brechbiel, M.J. Mattes, A comparison of 4 radionuclides conjugated to antibodies for single-cell kill, J. Nucl. Med. 44 (2003) 632–640.
[163] R.B. Michel, M.J. Mattes, Intracellular accumulation of the anti-CD20 antibody 1F5 in B-lymphoma cells, Clin. Cancer Res. 8 (2002) 2701–2713.
[164] R.B. Michel, A.V. Rosario, P.M. Andrews, D.M. Goldenberg, M.J. Mattes, Therapy of small subcutaneous B-lymphoma xenografts with antibodies conjugated to radionuclides emitting low-energy electrons, Clin. Cancer Res. 11 (2005) 777–786.
[165] J.L. Shipley, J.N. Butera, Acute myelogenous leukemia, Exp. Hematol. 37 (2009) 649–658.
[166] M. Tanimoto, D.A. Scheinberg, C. Cordon-Cardo, D. Huie, B.D. Clarkson, L.J. Old, Restricted expression of an early myeloid and monocytic cell surface antigen defined by monoclonal antibody M195, Leukemia 3 (1989) 339–348.
[167] J.M. Burke, P.C. Caron, E.B. Papadopoulos, C.R. Divgi, G. Sgouros, K.S. Panageas, R.D. Finn, S.M. Larson, R.J. O'Reilly, D.A. Scheinberg, J.G. Jurcic, Cytoreduction with iodine-131-anti-CD33 antibodies before bone marrow transplantation for advanced myeloid leukemias, Bone Marrow Transplant. 32 (2003) 549–556.
[168] J.G. Jurcic, P.C. Caron, T.K. Nikula, E.B. Papadopoulos, R.D. Finn, O.A. Gansow, W.H. Miller Jr., M.W. Geerlings, R.P. Warrell Jr., S.M. Larson, et al., Radiolabeled anti-CD33 monoclonal antibody M195 for myeloid leukemias, Cancer Res. 55 (1995) 5908–5910.
[169] V. Kersemans, B. Cornelissen, M.D. Minden, J. Brandwein, R.M. Reilly, Drug-resistant AML cells and primary AML specimens are killed by $^{111}$In-anti-CD33 monoclonal antibodies modified with nuclear localizing peptide sequences, J. Nucl. Med. 49 (2008) 1546–1554.
[170] D. Bonnet, J.E. Dick, Human acute myeloid leukemia is organized as a hierarchy that originates from a primitive hematopoietic cell, Nat. Med. 3 (1997) 730–737.
[171] F. Ishikawa, S. Yoshida, Y. Saito, A. Hijikata, H. Kitamura, S. Tanaka, R. Nakamura, T. Tanaka, H. Tomiyama, N. Saito, Chemotherapy-resistant human AML stem cells home to and engraft within the bone-marrow endosteal region, Nat. Biotechnol. 25 (2007) 1315–1321.
[172] N. Misaghian, G. Ligresti, L.S. Steelman, F.E. Bertrand, J. BÑsecke, M. Libra, F. Nicoletti, F. Stivala, M. Milella, A. Tafuri, M. Cervello, A.M. Martelli, J.A. McCubrey, Targeting the leukemic stem cell: the Holy Grail of leukemia therapy, Leukemia 23 (2009) 25–42.
[173] C.T. Jordan, D. Upchurch, S.J. Szilvassy, M.L. Guzman, D.S. Howard, A.L. Pettigrew, T. Meyerrose, R. Rossi, B. Grimes, D.A. Rizzieri, S.M. Luger, G.L. Phillips, The interleukin-3 receptor alpha chain is a unique marker for human acute myelogenous leukemia stem cells, Leukemia 14 (2000) 1777–1784.
[174] Q. Sun, J.M. Woodcock, A. Rapoport, F.C. Stomski, E.I. Korpelainen, C.J. Bagley, G.J. Goodall, W.B. Smith, J.R. Gamble, M.A. Vades, A.F. Lopez, Monoclonal antibody 7G3 recognizes the N-terminal domain of the human interleukin-3 (IL-3) receptor ‡ — chain and functions as a specific IL-3 receptor antagonist, Blood 87 (1996) 83–92.
[175] J.V. Leyton, M. Hu, C. Gao, P.V. Turner, J.E. Dick, M. Minden, R.M. Reilly, Auger electron radioimmunotherapeutic agent specific for the CD123$^+$/CD131$^-$ phenotype of the leukemia stem cell population, J. Nucl. Med. 52 (2011) 1465–1473.
[176] J.V. Leyton, B. Williams, C. Gao, A. Keating, M. Minden, R.M. Reilly, MicroSPECT/CT imaging of primary human AML engrafted into the bone marrow and spleen of NOD/SCID mice using $^{111}$In-DTPA-NLS-CSL360 radioimmunoconjugates recognizing the CD123$^+$/CD131$^-$ epitope expressed by leukemia stem cells, Leuk. Res. 38 (2014) 1367–1373.
[177] A. Zereshkian, J.V. Leyton, Z. Cai, D. Bergstrom, M. Weinfeld, R.M. Reilly, The human polynucleotide kinase/phosphatase (hPNKP) inhibitor A12B4C3 radiosensitizes human myeloid leukemia cells to Auger electron-emitting anti-CD123 $^{111}$In-NLS-7G3 radioimmunoconjugates, Nucl. Med. Biol. 41 (2014) 377–383.
[178] J.V. Leyton, C. Gao, B. Williams, A. Keating, M. Minden, R.M. Reilly, A radiolabeled antibody targeting CD123$^+$ leukemia stem cells - initial radioimmunotherapy studies in NOD/SCID mice engrafted with primary AML, Leuk. Res. Rep. 4 (2015) 55–59.

Please cite this article as: S. Aghevlian, et al., Radioimmunotherapy of cancer with high linear energy transfer (LET) radiation delivered by radionuclides emitting α-particles or ..., Adv. Drug Deliv. Rev. (2015), http://dx.doi.org/10.1016/j.addr.2015.12.003